Model Predictive Control of Sheet and Film Forming Processes

by

Jianfeng Zhang

A thesis submitted in partial fulfillment of

the requirements for the degree of

MASTER OF SCIENCE

(Chemical Engineering)

at the

UNIVERSITY OF WISCONSIN–MADISON

1997

Acknowledgments

I would first like to express my thanks and appreciation to my advisor, Professor James B. Rawlings. I am grateful to him for the opportunity of working in his research group and his insightful guidance for my work.

I would like to express my gratitude to the Rawlings research group: Rahul Bindlish, John C. Campbell, John W. Eaton, Claire E. Epley, Peter Findeisen, Rolf Findeisen, Hazel B. Matthews (Rock), Scott A. Middlebrooks, Daniel Patience, Chris Rao and Olav Slupphaug. They helped me much both academically and personally. Special thanks go to John Campbell for sharing his large experience in the area of gage control.

I would like to thank Ms. Becky Fisher of ESL and Miss Elizabeth Gannaway for their helpful comments on this thesis.

Finally, I am very grateful to my parents. They have always supported me in the pursuit of knowledge and made many sacrifices to ensure that I received a good education. I thank them for their moral and financial support over the years.

Abstract

The large-scale, uncertain, constrained nature of sheet and film processes makes their control especially interesting and challenging. The general problem of controlling both machine and cross-directional properties in sheet and film forming processes is treated in this thesis. A linear dynamic model capable of characterizing both the process and disturbance dynamics is used. A control scheme combining a time-varying Kalman filter, a constrained linear model predictive control and on-line model identification is constructed and evaluated. Simulation results demonstrate that the scheme can control the MD and the CD profiles simultaneously and good performance can be obtained where various types of disturbances, actuator faults and model mismatches occur in the systems.

Contents

Acknowledgments ii

Abstract iii

List of Figures vi

Chapter 1 Introduction 1

1.1 Process Characteristics 2

1.2 Literature Review 4

1.3 Organization 8

Chapter 2 Process Model 10

2.1 Linear Dynamics 10

2.2 Measurement Matrix 15

2.3 Disturbance and noise model 17

Chapter 3 The Control Problem 20

3.1 Model Predictive Control 20

3.2 Constraints 24

3.3 State Estimation 25

3.4 Nominal Stability 27

Chapter 4 Simulation Results **29**

Chapter 5 Lane Shift **44**

5.1 Lane Shift 44

5.2 Lane identification 49

5.3 Examples 57

Chapter 6 Conclusions **61**

Bibliography **65**

List of Figures

1.1 Schematic of film or sheet forming process. Taken from Campbell *et al.*[13]. 2

2.1 Schematic of film or sheet forming process with two scanning sensors. 15

4.1 Step disturbance rejection by using two scanning sensors 33

4.2 Step disturbance rejection by using one scanning sensor . 33

4.3 Closed-loop response of the output. 35

4.4 Closed-loop response of the MD profile. 35

4.5 Step disturbance rejection in the case of actuator bias, without measured inputs 36

4.6 Step disturbance rejection in the case of actuator break, without measured inputs 37

4.7 Step disturbance rejection in the case of actuator bias, with measured inputs 38

4.8 Step disturbance rejection in the case of actuator break, with measured inputs 39

4.9 Step disturbance rejection with model/plant mismatch (1) 41

4.10 Step disturbance rejection with model/plant mismatch (2) 42

5.1 Illustration of lane shift 45

5.2 Disturbance rejection with step disturbance, white noise and lane shift=0.5. 47

5.3 Disturbance rejection with step disturbance, white noise and lane shift=1. 48

5.4 distribution of errors when shift=0 51

5.5 Accumulated errors when shift=0, t=1:250 52

5.6 Accumulated errors when shift=0, t=251:1000 52

5.7 distribution of errors when shift=1 53

5.8 Accumulated errors when shift=1, t=1:250 54

5.9 Accumulated errors when shift=1, t=251:1000 54

5.10 Disturbance rejection with step disturbance, white noise and lane shift=1. 58

5.11 Disturbance rejection with step disturbance, white noise and lane shift=1. 58

5.12 Disturbance rejection with step disturbance, white noise and lane shift=0.8. 59

5.13 Disturbance rejection with step disturbance, white noise and lane shift=0.8. 59

5.14 Disturbance rejection with step disturbance, white noise and lane shift changes as a sinusoid function. 60

5.15 Disturbance rejection with step disturbance, white noise and lane shift changes as a sinusoid function. 60

Nomenclature

A, B, C	state-space model matrices
$\hat{A}, \hat{B}$	augmented state-space model matrices
$\tilde{A}, \tilde{B}, \tilde{C}$	augmented state-space model matrices
D	adjacent actuator constraint matrix
$d_{\min}, d_{\max}$	minimum, maximum adjacent actuator constraint vector
E	error matrices
G	state noise dynamics matrix
$\tilde{G}$	augmented state noise dynamics matrix
K	steady-state actuator gain matrix
k	time index
L	Kalman filter gain matrix
l	number of lanes
M	tuning parameter in lane identification
N	regulator horizon length
P	filtering Riccati matrix

p	output disturbance
p	period of scanning sensor
Q	output penalty matrix
Q_ω	covariance matrix of ω
$\bar{Q}$	terminal state penalty matrix
R	input penalty matrix
R_ν	covariance matrix of ν
S	input rate of change penalty matrix
u	input vector
$\hat{u}, \tilde{u}$	augmented input vector
$\bar{u}$	desired input vector
$u_{\min}, u_{\max}$	minimum, maximum input constraint vector
W	length of identification horizon
v	input vector
x	state vector
$\tilde{x}$	augmented state vector
$\hat{x}$	estimated state vector
y	output vector
y_t	setpoint vector
$y_{\min}, y_{\max}$	minimum, maximum output constraint vector
z	input disturbance

Δu	change in the input vector
$\Delta u_{\min}, \Delta u_{\max}$	min, max input rate of change constraint vector
Φ	regulator objective function
π	input vector decision variables
τ	time delay
ν	zero-mean, normal output noise vector
ω	zero-mean, normal state noise vector
ξ	zero-mean, normal disturbance state noise vector

Chapter 1

Introduction

The identification and control of sheet and film forming processes, which are used to manufacture many different types of polymer films and paper sheets, continue to draw attention from industry and university researchers. Improved control of sheet and film properties can mean higher product quality, greater production rate, and significant savings in energy and raw materials. A great deal of research has been conducted on sheet and film forming processes in the last few decades. However, the characteristics of such processes make effective control difficult. Such characteristics include inaccurate process models, large numbers of actuators and sensing locations, significant time delays, periodic and noisy sensors, actuator constraints, equipment faults, lane shifts, and other uncertain disturbances. Among other strategies, Model Predictive Control (MPC) technology has been applied for these processes. The power of MPC, including its ability to handle constraints, makes this technology a good candidate for industrial implementation. Based on former research results, this thesis proposes some new methods to model and control the processes and studies some types of disturbances that have not been considered before.

1.1 Process Characteristics

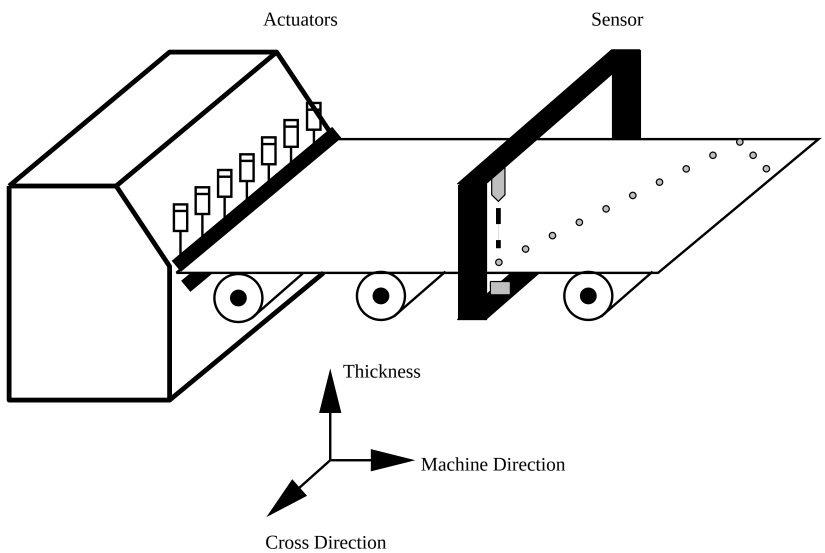

Figure 1.1: Schematic of film or sheet forming process. Taken from Campbell *et al.*[13].

Figure 1.1 depicts the main features of a generic film forming process. There is an area at which the film is extruded through a row of actuators and then pinned to roller conveyers. The film is then conveyed along the rollers through a process that involves stretching, heating, drying, shrinking, and setting. Before the film is wound up on a drum as the final product, one or more sensors measure the related properties of the film. A scanning sensor, which scans back and forth over the film while the film is moving underneath it, is usually used. This twofold movement provides measurements in a zig-zag pattern along the sheet.

The following terms are commonly used in the literature. The machine direction (MD) refers to the direction in which the film is conveyed. The cross direction (CD) refers to the direction that is perpendicular to the machine direction across the film. A lane refers to a particular cross direction location. The sample time refers to the time interval at which the sensor provides its information. The time delay is the number of sample times between the time the film passes through the actuator and the time it arrives at the sensor's machine direction location.

The sheet or film properties, such as the film gage (another name for thickness), vary both in machine direction and in cross direction. It is common to assume that the property variations about a mean can be separated into three components: an MD term, a CD term, and a residual term. Furthermore, the variances of these three terms are often assumed to be independent from one another, and the MD and the CD components are controlled separately. In order to control the MD variations, it is usual to control the total flowrate of material into the die or headbox. Generally, the effect of a flowrate change is to raise or lower the film property uniformly across the film, that is, it changes the average level of profile, but not the shape of the profile. To control the CD profile variations, a row of actuators is placed as shown in Figure 1.1.

Current industrial practice is far from optimal due to limitations in the sensor and control technologies that are used. The characteristics that make effective control of sheet and film processes especially difficult are summarized by Braatz *et al.* [9]:

Large-Scale Sheet and film processes can have up to 100 actuators and hundreds of sensing locations. The large-scale and high speed nature of these processes put serious constraints on the amount of on-line computation available for the control algorithm.

Plant/Model Mismatch It is impossible to generate a highly accurate sheet and film process model because of: lack of complete understanding of the underlying physical phenomena; inaccurate values for the physical parameters of the sheet and film process; cross-directional movement of the entire sheet or film web; and unknown disturbances.

Faults and Failures Equipment faults and failures are common during normal sheet and film process operations.

Constraints Actuator positions for sheet and film processes are usually constrained.

Scanning Sensors Due to the high cost of sensors, scanning sensors are usually used, as illustrated in Fig. 1.1.

1.2 Literature Review

The process control problem for sheet and film processes is typically separated into two main control objectives: the machine-direction (MD) control problem and the cross-directional (CD) control problem. The MD control problem, which is the maintenance of the average sheet or film thickness, has been studied extensively since the application of stochastic control to the problem by Åström in the late 1960s [2]. A survey of the early work on MD control is provided by Brewster and Bjerring [11], and a survey of later work is presented by Dumont [19]. The CD control problem, which is to maintain flat profiles across the machine, is much more difficult than the MD problem, and has recently drawn significant attention from industry and academia. A critical review of recent work on the CD control problem is provided by Braatz *et al.* [9]. The simultaneous MD and CD control is also reported [6], and seems to be a trend in recent research.

A number of linear and non-linear models that relate the actuator movement to the gage properties have been proposed in the literature. Åström [2] uses a linear first order ARMAX model identified from process data. Wang, Dumont, and Davies [37] propose a more complex non-linear statistical model that couples the machine direction and cross direction variations of the sheet properties in order to estimate the variances in either direction. An impulse response model that handles large time delays is used by Xia, Rao and Qian [40]. Recently, steady-state models, which assume that the dynamics of the process due to actuator movement can be neglected, are usually used. Boyle [7] provides a brief discussion and Wilhelm Jr. and Fjeld [38] elaborate on the diagonally dominant steady-state gain matrix model. Wilkinson and Hering [39] suggest a self tuning or updating gain matrix that could be considered to be a time-varying steady-state model. The symmetry characteristics of these steady state models are discussed by Braatz *et al.* [9]. An identification method based on the inherent symmetry in these processes is proposed by Campbell and Rawlings [15].

The scanning sensor raises an interesting state estimation problem. Filtering techniques that decouple the machine direction variations and the cross direction variations are presented by Chen [16]. Dumont *et al.* [20] estimate the cross direction moisture content profile on-line via a Kalman filtering method in conjunction with an exponential forgetting and resetting version of a recursive least-squares algorithm. This algorithm updates the current lane and adjacent lane values of moisture content with each measurement. Bergh and MacGregor [6] point out the idea of using a time-varying C matrix in conjunction with a Kalman filter for this process. Rawlings and Chien [31] elaborate on this idea and show how the covariance of the estimates can be used to evaluate different scanning patterns. Presented by Tyler and Morari [35] is the discussion of differences between scanning and fixed sensors.

A wide variety of control strategies for sheet and film process appear in the literature. The two CD control schemes reported in the literature before 1988 were linear-quadratic-optimal(LQ) [6, 8, 38] and model inverse-based control [5]. Mostly used were steady state models. One weakness of these linear control approaches is that constraints can be satisfied only by sufficiently penalizing the control action in the objective function, thus making the control action sluggish. Recently, the application of Model Predictive Control has been considered for the control of paper machines, coating process, and polymer film extruders. Boyle [7, 8] first proposed solving a quadratic program to handle hard actuator constraints on a steady-state process model. Wang, Dumont and Davies [36] use generalized prediction control (GPC) to control the machine direction variations of paper basis weight. They are able to take into account the time-delay, but do not address constraints. Braatz *et al.* [10] assume a stationary bank of sensors and scale the input in order to handle input constraints and avoid controller wind up. Rawlings *et al.* [17, 14, 15] formulated a time-varying Kalman filter to estimate full film properties and designed an MPC approach that can handle hard constraints. Using measured inputs as a method to detect actuator faults is discussed by Campbell and Rawlings [15] as well. Arkun *et al.* [1] use Karhunen-Loeve expansion to adaptively identify the significant features of the sheet profile and develop reduced order models for the model predictive control algorithm. Kristinsson and Dumont [25] use orthogonal polynomials to optimize the shape of the slice lip to best control the cross directional variations. Although this method does handle constraints, it is not a predictive controller.

One advantage of model predictive control for the sheet and film process is handling the hard constraints on the actuators. Accounting for constraints can improve robustness, handle failed actuators and prevent stress on the die lip by limiting the motion of neighboring actuators. Nominal stability properties of the constrained, linear and nonlinear regulator are presented by Rawlings *et al.* [29, 34, 14]. Believing that the MPC controller can improve the control quality, this thesis will present the performance of the MPC controller under important combinations of possible disturbances, and anticipate its practicability in industry. In addition, we consider new methods that may improve the control. Such methods include using an additional scanning sensor, measuring inputs, controlling the MD and CD variations simultaneously, and using on-line identification.

1.3 Organization

This thesis is subdivided according to the following structure:

Chapter 1 Introduction.

Chapter 2 Construction of the simplest mathematical model that can describe many of the known process characteristics. Time-varying measurement matrix and disturbance models are discussed.

Chapter 3 Introduction of the concepts of receding horizon linear model predictive control and time-varying Kalman filter estimation. Hard constraints in the sheet and film forming processes and nominal stability of the control scheme is also introduced.

Chapter 4 Presentation of some simulation results of gage control implementation. Simultaneous MD and CD control, actuator faults, model mismatch are illustrated.

Chapter 5 Construction of an on-line identification method. The effect of lane shift is first introduced. Several simulation examples are given to demonstrate the scheme.

Chapter 6 Conclusions.

Chapter 2

Process Model

The purpose of this chapter is to provide the simplest mathematical model that can describe the essential features of the process. Due to the complex mechanics involved in the process, it is impractical to obtain a first principles model. However, because of the nature of feedback control, an extremely accurate model is not necessary in order for the controller to provide acceptable closed-loop performance. Thus, an empirical linear model can be chosen to simplify the modeling.

2.1 Linear Dynamics

The final sheet or film thickness can be affected by many variables. It is common to separate the thickness variations into to two parts: the MD part and the CD part. The machine direction variations may arise from changes in drier steam pressure, changes in machine speed, etc. The cross-directional variations may arise from stock flow distribution across the slice, changes in wire conditions, etc. These two variations are traditionally assumed to be independent of one another and are controlled separately. In this thesis, the MD and CD components are simultaneously controlled by one MPC controller, based on the fact that the MD and CD variations are dependent on one another. The MD control is just an extension of the CD control by using additional actuator(s). According to Bergh and Macgregor [6], the input (scalar or vector) used to control the MD component is called the *lumped input*, which adjusts the average level of profile but not the shape of the profile, while the input vector used to control the cross-directional variations is called the *local input*.

An empirical assumption is that the major dynamics in sheet forming processes usually occur in the machine direction between the lumped input and the response at any position. Thus we can use a steady-state gain model to relate the local input to the CD profile and consider dynamics only in the machine direction.

Many studies have been performed to identify discrete transfer function models that relate the lumped input v to the MD component (average thickness) x_m. Discrete transfer function models of the form

$$\begin{aligned} x_m(k) &= \frac{(\omega_0 - \omega_1 z^{-1} - \ldots - \omega_s z^{-s})}{1 - \delta_1 z^{-1} - \ldots - \delta_r z^{-r}} \cdot v(k) \\ &= G_v(z^{-1}) v(k) \end{aligned}$$

with low orders ($s, r \leq 2$) are usually found to be adequate [6]. Here, z^{-1} is the backward shift operator ($z^{-1} v_t = v_{t-1}$), $\omega_0 \ldots \omega_s$, and $\delta_1 \ldots \delta_r$

are coefficients. In this study, we use the state space model

$$x_m(k+1) \quad = \quad A_m x_m(k) + B_m v(k-\tau_1) \tag{2.1}$$

where τ_1 is a time delay.

In the cross direction, the sheet is divided up into n lanes and m local actuators are used to control these lanes. Modeling the effect of local actuator manipulations on the expected cross-directional responses has been discussed in several papers [2, 24]. In many applications the dynamics caused by actuator movement are negligible compared to the scanning frequency further down the sheet. This assumption leads to a steady-state gain model that relates actuator position to film thickness. In discrete time, this model has the form

$$x_c(k+1) \quad = \quad B_c u(k-\tau_2) \tag{2.2}$$

Here x_c is the vector of the cross direction component of the film thickness caused by u, with u as the vector of local actuator positions, and τ_2 as the time delay.

Neglecting the noise term, the vector of film thickness is given by:

$$x(k) \quad = \quad x_m(k) + x_c(k) \tag{2.3}$$

Considering that x_m represents the average thickness of x, we can combine the above models as

$$x(k+1) \quad = \quad Ax(k) + Bv(k-\tau_1) + Ku(k-\tau_2) \tag{2.4}$$

Time delays are handled by enlarging the state. Either past states or past inputs can be stored. Because the input vector often has a smaller dimension than the state vector, past inputs are used to enlarge the state. A state-space model without time delay for the enlarged state can be constructed as

$$\hat{x}(k+1) = \hat{A}\hat{x}(k) + \hat{B}\hat{u}(k) \tag{2.5}$$

where

$$\hat{x}(k) = \begin{bmatrix} x(k) \\ v(k-\tau_1) \\ \vdots \\ v(k-2) \\ v(k-1) \\ u(k-\tau_2) \\ \vdots \\ u(k-2) \\ u(k-1) \end{bmatrix}$$

and

$$\hat{u}(k) = \begin{bmatrix} v(k) \\ u(k) \end{bmatrix}$$

It is common for a scanning sensor to be installed just before the film is wound up on a roll. There is often a significant time delay between the actuators and the sensor, whereas disturbances may occur throughout the process. In this study, an additional scanning sensor is used to improve estimation and detect some disturbances at an earlier stage. This additional sensor is assumed to be installed near the local actuators so that it can quickly detect disturbances from upstream sources and actuator faults. A more complex model would therefore be given by:

$$\begin{aligned} \tilde{x}(k+1) &= \tilde{A}\tilde{x}(k) + \tilde{B}\tilde{u}(k) \\ y(k) &= \tilde{C}(k)\tilde{x}(k) \end{aligned} \tag{2.6}$$

where

$$\tilde{x}(k) = \begin{bmatrix} x_1(k) \\ x_2(k) \\ v(k-\tau_1) \\ \vdots \\ v(k-2) \\ v(k-1) \\ u(k-\tau_2) \\ \vdots \\ u(k-2) \\ u(k-1) \end{bmatrix}$$

and

$$\tilde{u}(k) = \begin{bmatrix} v(k) \\ u(k) \end{bmatrix}$$

In this model x_1 is the vector of film thickness at the casting position (See Figure 2.1), x_2 is the vector of film thickness at the wind-up position, v is the vector (or scalar) of lumped input(s), u is the vector of local actuator positions, y is the vector of sensor measurements, τ_1

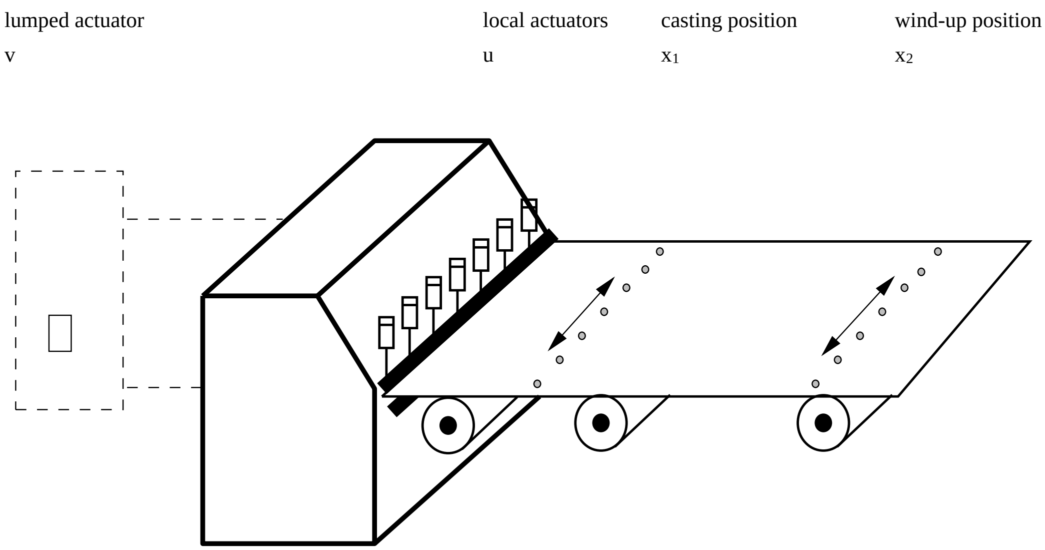

Figure 2.1: Schematic of film or sheet forming process with two scanning sensors.

is the time delay between the lumped input and the wind-up position, and τ_2 is the time delay between the local actuators and the wind-up position. Vector u has a length equal to the number of local actuators and vector y has a length equal to the number of sensors. Vectors x_1 and x_2 have lengths equal to the number of measurement positions. Because the film is stretched in the process, it is not necessary for vector x_1 to have the same length as x_2.

2.2 Measurement Matrix

Because scanning sensors are used, each sensor measures only one lane at each sample time. Therefore, the C matrix is a time-varying matrix in equation 2.6. Rawlings and Chien showed how the moving sensor could be described with a time-varying C matrix [31]. This idea is due to Bergh and MacGregor [6].

First let us consider a simple example to make this clear. Here only one scanning sensor which scans five positions periodically is used. Consider

$$y(k) = C(k)x(k)$$

where $y(k)$ represents the output of the sensor at time k and $x(k)$ represents the vector of film thickness with length 5. Assume that at time 1, the sensor is above the first lane; then the pattern of scanning is represented by

$$\begin{aligned}
y(1) &= \begin{bmatrix} 1 & 0 & 0 & 0 & 0 \end{bmatrix} x(1) \\
y(2) &= \begin{bmatrix} 0 & 1 & 0 & 0 & 0 \end{bmatrix} x(2) \\
y(3) &= \begin{bmatrix} 0 & 0 & 1 & 0 & 0 \end{bmatrix} x(3) \\
y(4) &= \begin{bmatrix} 0 & 0 & 0 & 1 & 0 \end{bmatrix} x(4) \\
y(5) &= \begin{bmatrix} 0 & 0 & 0 & 0 & 1 \end{bmatrix} x(5) \\
y(6) &= \begin{bmatrix} 0 & 0 & 0 & 1 & 0 \end{bmatrix} x(6) \\
y(7) &= \begin{bmatrix} 0 & 0 & 1 & 0 & 0 \end{bmatrix} x(7) \\
y(8) &= \begin{bmatrix} 0 & 1 & 0 & 0 & 0 \end{bmatrix} x(8)
\end{aligned}$$

This pattern then repeats and

$$\begin{aligned}
y(9) &= \begin{bmatrix} 1 & 0 & 0 & 0 & 0 \end{bmatrix} x(9) \\
&\vdots
\end{aligned}$$

Clearly $C(k)$ is a time-varying, periodic, row vector with period 8.

In general, let l be the number of sensed lanes, p be the period of the scanner, and

$$r = 1 + (k-1) \bmod 2(\mathrm{l}-1)$$

Then $C(k)$ is a row vector of zeros except for a one in the qth location in which

$$\begin{array}{lll} q = r, & 1 \leq r \leq l-1, & \text{forward sensor sweep} \\ q = 2l - r, & l \leq r \leq 2(l-1), & \text{return sensor sweep} \end{array}$$

and

$$p = 2(l-1)$$

It is straightforward to extend this description to the enlarged state equation with multiple scanning sensors. In the case of multiple scanning sensors, each of which has a scanning period, the period of the C matrix in equation 2.6 equals the least common multiple of these individual periods.

2.3 Disturbance and noise model

In order for a controller to perform good disturbance rejection, the controller should include an integrating disturbance model. The presence of integral action can remove steady-state offset caused by step disturbances or mismatch between the plant and the model [29, 31].

The most common method for obtaining integral action in the controller is to use an output disturbance model. This model can be represented by augmenting the system with a vector of additional states, p, which represents the output disturbance.

$$\begin{aligned} x_{k+1} &= Ax_k + Bu_k \\ p_{k+1} &= p_k \\ y_k &= Cx_k + p_k \end{aligned} \tag{2.7}$$

Another popular integrating disturbance model is the so-called input disturbance model, which can be represented by augmenting the system with a vector of additional states, z, to represent the input disturbance.

$$\begin{aligned} x_{k+1} &= Ax_k + B(u_k + z_k) \\ z_{k+1} &= z_k \\ y_k &= Cx_k \end{aligned} \tag{2.8}$$

If we append both disturbance states and stochastic variables to the plant model, the augmented state equations can be represented as

$$\underbrace{\begin{bmatrix} x_{k+1} \\ p_{k+1} \\ z_{k+1} \end{bmatrix}}_{\tilde{x}_{k+1}} = \underbrace{\begin{bmatrix} A & 0 & G_z \\ 0 & I & 0 \\ 0 & 0 & I \end{bmatrix} \begin{bmatrix} x_k \\ p_k \\ z_k \end{bmatrix}}_{\tilde{A}\tilde{x}_k} + \underbrace{\begin{bmatrix} B \\ 0 \\ 0 \end{bmatrix} u_k}_{\tilde{B}u_k} + \underbrace{\begin{bmatrix} G_w & 0 & 0 \\ 0 & G_\xi & 0 \\ 0 & 0 & G_\omega \end{bmatrix} \begin{bmatrix} w_k \\ \xi_k \\ \omega_k \end{bmatrix}}_{\tilde{G}_{\tilde{w}}\tilde{w}_k} \tag{2.9}$$

$$
\begin{aligned}
\underbrace{y_k}_{} &= \underbrace{\begin{bmatrix} C(k) & G_p & G_z \end{bmatrix}}_{} \underbrace{\begin{bmatrix} x_k \\ p_k \\ z_k \end{bmatrix}}_{} + \underbrace{\nu_k}_{} \\
y_k &= \qquad \tilde{C}(k) \qquad\qquad \tilde{x}_k \quad + \; \nu_k
\end{aligned}
$$

In this representation, p_k is output disturbance vector, z_k is input disturbance vector, and $w_k, \xi_k, \omega_k, \nu_k$ are zero-mean normally distributed stochastic noise variables. This framework allows for a great deal of flexibility in representing a disturbance model for the process. However, the combined number of states in the p and z vectors cannot be greater than the number of outputs [29]. This limitation is because of the observability requirement that the augmented disturbance states must be able to be estimated from the output measurements. Detailed discussion of this issue can be found in Muske's PhD thesis [28]. In many cases either of these two disturbance models can provide adequate performance in the face of several types of disturbances. In the case where actuator positions are measured, both input and output disturbances can be included in the model to efficiently reject various types of disturbances.

Chapter 3

The Control Problem

This chapter deals with the gage control algorithm. In the first section, the model predictive control concept is reviewed with emphasis on constrained receding horizon MPC. In section 2, constraints are discussed. The state estimation problem is introduced in section 3, and stability is discussed in section 4.

3.1 Model Predictive Control

Model Predictive Control (MPC) refers to a class of computer control schemes that utilize a process model to explicitly predict future plant behavior and compute appropriate control action by solving an optimization problem on-line at each control execution. Process input and output constraints are included directly in the optimization problem so that future constraint violations are prevented. The MPC technology is particularly easy to use for multivariable systems and for handling process interactions, time delays, and other difficult process dynamics.

Incorporation of process constraints makes MPC technology extremely powerful. It has been applied successfully to a large number of processes in various industries. A more complete discussion of earlier model predictive control implementations is contained in the review articles by De Keyser *et al.* [18], Byun and Kwon [13], and Garcia *et al.* [22]. Recent reviews include the papers of Muske and Rawlings [29], Rawlings *et al.* [32], Mayne [27], Qin and Badgwell [30], and Lee [26]. The differences between these implementations are in the form of the model and performance objective, the choice of horizon, and the tuning parameters. What we utilize in the gage control problem is the Receding Horizon Regulator algorithm that is extensively discussed in the paper of Muske and Rawlings [29].

The receding horizon regulator is based on the minimization of the following infinite horizon open-loop quadratic objective function at time k.

$$\min_{\pi} \sum_{j=0}^{\infty} \left(y_{k+j}^T Q y_{k+j} + u_{k+j}^T R u_{k+j} + \Delta u_{k+j}^T S \Delta u_{k+j} \right) \qquad (3.1)$$

Here Q is a symmetric positive semidefinite penalty matrix on the outputs with y_{k+j} computed from the process model. R is a symmetric positive definite penalty matrix on the inputs in which u_{k+j} is the input vector at time j in the open-loop objective function. S is a symmetric positive semidefinite penalty matrix on the rate of change of the inputs in which $\Delta u_{k+j} = u_{k+j} - u_{k+j-1}$ is the change in the input vector at time j. The vector π contains the N future open-loop control moves as shown below.

$$\pi = \begin{bmatrix} u_k \\ u_{k+1} \\ \vdots \\ u_{k+N-1} \end{bmatrix} \tag{3.2}$$

The input vector is finitely parameterized by setting $u_{k+j} = 0$ for all $j \geq N$.

The receding horizon regulator computes the vector π that optimizes the open-loop objective function in Equation 3.1. The first input value in π, u_k, is then injected into the plant as the real input. This procedure is repeated at each successive control interval with feedback incorporated by using the plant measurements to update the state vector at time k. With this feedback, the regulator can be applied when an exact model is not available.

The infinite horizon objective function in Equation 3.1 can be expressed as the finite horizon objective function shown below.

$$\begin{aligned} \min_{\pi} \Phi_k &= \sum_{j=0}^{N-1} \left(y_{k+j}^T Q y_{k+j} + u_{k+j}^T R u_{k+j} + \Delta u_{k+j}^T S \Delta u_{k+j} \right) \\ &\quad + y_{k+N}^T \bar{Q} y_{k+N} \end{aligned} \tag{3.3}$$

Determination of the terminal state penalty matrix, $\bar{Q}$, is proposed by Muske and Rawlings [29].

The above regulator is for a zero target. In gage control, we want the controller to have the ability to track step changes in a nonzero output target vector, y_t; thus the control calculation is split into a steady-state optimization followed by a dynamic optimization. Optimal steady-state targets are computed for each state and input; these are then passed to a dynamic optimization to compute the optimal input vector. The steady-state state and input vectors, x_s and u_s, are determined by the following quadratic program.

$$\begin{aligned} \min_{[x_s,u_s]^T} \Psi &= (y_t - Cx_s)^T Q_s (y_t - Cx_s) \\ &+ (u_s - \bar{u})^T R_s (u_s - \bar{u}) \end{aligned} \tag{3.4}$$

subject to:

$$\begin{bmatrix} I - A & -B \end{bmatrix} \begin{bmatrix} x_s \\ u_s \end{bmatrix} = 0 \tag{3.5}$$

$$u_{min} \le u_s \le u_{max} \tag{3.6}$$

In this quadratic program, $\bar{u}$ is the desired value of the input vector at steady state and Q_s, R_s are positive definite weighting matrices for the output tracking error and the deviation of the input vector from $\bar{u}$, respectively. A steady-state solution is guaranteed by the equality constraints in Eq. 3.5. The input constraints are represented in Inequality 3.6.

This quadratic program in Eq. 3.4 is similar to that in Muske and Rawlings' paper. The difference is that they solve two different quadratic programs and do not include input penalties when there are not enough degrees of freedom to track the output target vector without offset. In some processes [10], the thicknesses x are not uniquely determined by the inputs u. Therefore, in gage control, the B matrix may be singular, making input penalties necessary.

In gage control, we often use an augmented model to deal with time delays. Because the quadratic program in Eq. 3.4 is to find the steady state solution, the time delay can be dropped in this step and the calculation speed can be improved.

Then, the following quadratic objective function is used to compute the optimal input vector.

$$\begin{aligned} \min_{\pi} \Phi \;=\; & (x_{k+N} - x_s)^T \bar{Q} (x_{k+N} - x_s) + \Delta u_{k+N}^T S \Delta u_{k+N} \\ & + \sum_{j=0}^{N-1} \left[(x_{k+j} - x_s)^T C^T Q C (x_{k+j} - x_s) \right] \\ & + \sum_{j=0}^{N-1} \left[(u_{k+j} - u_s)^T R (u_{k+j} - u_s) + \Delta u_{k+j}^T S \Delta u_{k+j} \right] \end{aligned} \tag{3.7}$$

If the process model contains no dynamics, that is, $A = 0$, then the above quadratic problem is not necessary, because the solution is the steady state u_s in Eq. 3.4. Without this step, if A does not equal to zero matrix, a sluggish trajectory is expected. Time delay can be dropped from the model by shifting the initial conditions.

3.2 Constraints

Actuator positions for sheet and film processes are usually constrained. If the regulator does not account for these constraints, small disturbances or process model errors may lead to large decreases in control performance [31]. The ability to handle constraints makes model predictive control an attractive method. Input and output constraints of the following form are usually considered.

$$
\begin{aligned}
u_{\min} &\leq u(j) \leq u_{\max}, & j &= 0, 1, \ldots, N-1 \\
y_{\min} &\leq y(j) \leq y_{\max}, & j &= j_1, j_1+1, \ldots, j_2 \\
\Delta u_{\min} &\leq \Delta u(j) \leq \Delta u_{\max}, & j &= 0, 1, \ldots, N-1
\end{aligned}
\tag{3.8}
$$

The output constraints are enforced from j_1 to j_2. These parameters need to be chosen to ensure feasibility; a method of calculation is proposed by Rawlings and Muske [33].

In film and sheet forming processes, another important kind of constraint is the one imposed to prevent the actuators from creating excess stress in the die or slice lip. This can be expressed as a limit on the difference between adjacent actuator positions,

$$d_{\min} \leq Du(j) \leq d_{\max} \tag{3.9}$$

where $d_{\min} = -d_{\max}$ are vectors of dimension $m-1$ (where m is the number of inputs) and

$$D = \begin{bmatrix} 1 & -1 & 0 & 0 & 0 \\ 0 & 1 & -1 & 0 & 0 \\ \vdots & \ddots & \ddots & \ddots & \vdots \\ 0 & 0 & 0 & 1 & -1 \end{bmatrix} \tag{3.10}$$

3.3 State Estimation

In recognition of the fact that no model can constitute a perfect representation of reality, it is necessary for the predictive control regulator to incorporate feedback to update the state predictions. The state estimation problem, also called the filtering problem, is to estimate the current states from the given model and available plant measurements. Two main filtering schemes employed in sheet and film forming processes are the first-order filter and the Kalman filter. The superiority of the Kalman filter to the first-order filter scheme is discussed by Rawlings and Chien [31]. The Kalman filter scheme is called *optimal state estimation* because it is designed to find the most likely value of the state from the output measurement and the given statistics of the random disturbances to the process. The following are brief descriptions of the key features of the Kalman filter. Further details are available in numerous books on stochastic control and optimal filtering (Bryson and Ho [12]; Åström [3]).

Consider the state-space model with scanning sensor and Gaussian noise,

$$\begin{aligned} x(k+1) &= Ax(k) + Bu(k) + G\omega(k) \\ y(k) &= C(k)x(k) + \nu(k) \end{aligned} \tag{3.11}$$

where ω and ν are zero-mean Gaussian random variables with covariances, Q_ω and R_ν respectively. The optimal estimate of x, $\hat{x}$, is provided by

$$\hat{x}(k+1|k) = A\hat{x}(k|k-1) + Bu(k) + L(k)\left(y(k) - C\hat{x}(k|k-1)\right) \tag{3.12}$$

The filter gain matrix, $L(k)$, can be computed efficiently in terms of the estimate error covariance matrix, $P(k)$,

$$L(k) = AP(k)C(k)^T \left[C(k)P(k)C(k)^T + R_v\right]^{-1} \tag{3.13}$$

where $P(k)$ can be computed from the following Riccati equation,

$$\begin{aligned} P(k+1) &= AP(k)A^T + GQ_\omega G^T \\ &\quad -AP(k)C(k)^T \left[C(k)P(k)C(k)^T + R_\nu\right]^{-1} C(k)P(k)A^T \end{aligned} \tag{3.14}$$

$P(k)$ is the covariance of the estimate error and provides a quantitative means for evaluating the quality of the estimate [31]. $L(k)$ and $P(k)$ will change periodically as k increases [14].

3.4 Nominal Stability

Nominal asymptotic stability of the closed-loop system presented in Section 3.1 is demonstrated by Muske *et al.* [33, 28, 34]. Since the input is determined from the solution of a quadratic program, the receding horizon regulator is nonlinear. Consequently, the standard linear system techniques used to demonstrate asymptotic stability are not appropriate. Asymptotic stability for this system is demonstrated by showing that the closed-loop state trajectory converges to the origin and the that the origin is stable. Convergence is demonstrated by showing that the optimal objective function value of the receding horizon quadratic program is monotonically convergent and that the objective function is a Lyapunov function for the closed-loop system. Stability properties of the combined time-varying Kalman filter and constrained, nonlinear regulator are discussed by Campbell and Rawlings [14] and asymptotic stability of the interconnected estimator and regulator is established. Rigorous description and proof is tedious and can be found in the references.

Chapter 4

Simulation Results

In this chapter some examples are provided to illustrate the performance of the MPC controller, which is applied for the process in Figure 2.1. The process is modeled by:

$$\begin{aligned} x_1(k+1) &= A_1x_1(k) + B_1v(k-3) + K_1u(k-1) \\ x_2(k+1) &= A_2x_1(k) + B_2v(k-3-\tau) + K_2u(k-1-\tau) \quad (4.1) \\ y_1(k) &= x_1(k) + p_1(k) \\ y_2(k) &= x_2(k) + p_2(k) \end{aligned}$$

$$A_1 = \begin{bmatrix} 0.176 & 0.176 & 0.176 & 0.176 & 0.176 \\ 0.176 & 0.176 & 0.176 & 0.176 & 0.176 \\ 0.176 & 0.176 & 0.176 & 0.176 & 0.176 \\ 0.176 & 0.176 & 0.176 & 0.176 & 0.176 \\ 0.176 & 0.176 & 0.176 & 0.176 & 0.176 \end{bmatrix}$$

$$B_1 = \begin{bmatrix} 1 \\ 1 \\ 1 \\ 1 \\ 1 \end{bmatrix}$$

$$K_1 = \begin{bmatrix} 4 & -1 & -1 & -1 & -1 \\ -1 & 4 & -1 & -1 & -1 \\ -1 & -1 & 4 & -1 & -1 \\ -1 & -1 & -1 & 4 & -1 \\ -1 & -1 & -1 & -1 & 4 \end{bmatrix}$$

$$A_2 = \begin{bmatrix} 0.146 & 0.146 & 0.146 & 0.146 & 0.146 & 0.146 \\ 0.146 & 0.146 & 0.146 & 0.146 & 0.146 & 0.146 \\ 0.146 & 0.146 & 0.146 & 0.146 & 0.146 & 0.146 \\ 0.146 & 0.146 & 0.146 & 0.146 & 0.146 & 0.146 \\ 0.146 & 0.146 & 0.146 & 0.146 & 0.146 & 0.146 \\ 0.146 & 0.146 & 0.146 & 0.146 & 0.146 & 0.146 \end{bmatrix}$$

$$B_2 = \begin{bmatrix} 5/6 \\ 5/6 \\ 5/6 \\ 5/6 \\ 5/6 \\ 5/6 \end{bmatrix}$$

$$K_2 = \begin{bmatrix} 0.833 & 0.111 & -0.278 & -0.333 & -0.333 \\ 0.500 & 0.389 & -0.222 & -0.333 & -0.333 \\ -0.333 & 0.500 & 0.500 & -0.333 & -0.333 \\ -0.333 & -0.333 & 0.500 & 0.500 & -0.333 \\ -0.333 & -0.333 & -0.222 & 0389 & 0.500 \\ -0.333 & -0.333 & -0.278 & 0.111 & 0.833 \end{bmatrix}$$

In this model y_1 is the vector of film thickness at the casting position (five lanes), y_2 is the vector of film thickness at the wind-up position (six lanes), p_1, p_2 are disturbances, v is a scalar representing the lumped input, u is the vector of local inputs with a length of five. The input v is used to control the average thickness of the film, while the input u only affects the shape in the cross direction. The variable τ represents the time delay between the casting position and the wind-up position.

The above model is augmented by the method described in Chapter 2. Unless otherwise specified, we assume no input is measured and the output disturbance model in Eq. 2.7 is used. We use the `lmpc` toolbox under `octave` [21] to do the simulation. The `lmpc` code was developed by Muske and Campbell. The code runs under MATLAB with the optimization toolbox, and under `octave` with the `qpsol` optimization routines. The code provides an easy way to experiment with constrained model predictive control. Disturbances, state feedback, and model mismatch can be investigated with the routines.

Example 4.1 First we consider an example containing a step disturbance. The process is described as equation 4.1 where $\tau = 40$. At time 10, a step disturbance occurs at lane 4 of the casting position ($p_1 = [0\ 0\ 0\ 0.5\ 0]^T$). Figure 4.1 shows the closed-loop response of the outputs. For comparison, Figure 4.2 shows the closed-loop response of the outputs for the same process while the casting-position sensor is not used. These two figures show that the additional sensor can improve the profile quality by detecting disturbances occurring at the early stage of the process. The bigger the time delay between the two sensors, the more advantages it will have. In the following examples, we use the model described in equation 4.1 with $\tau = 10$.

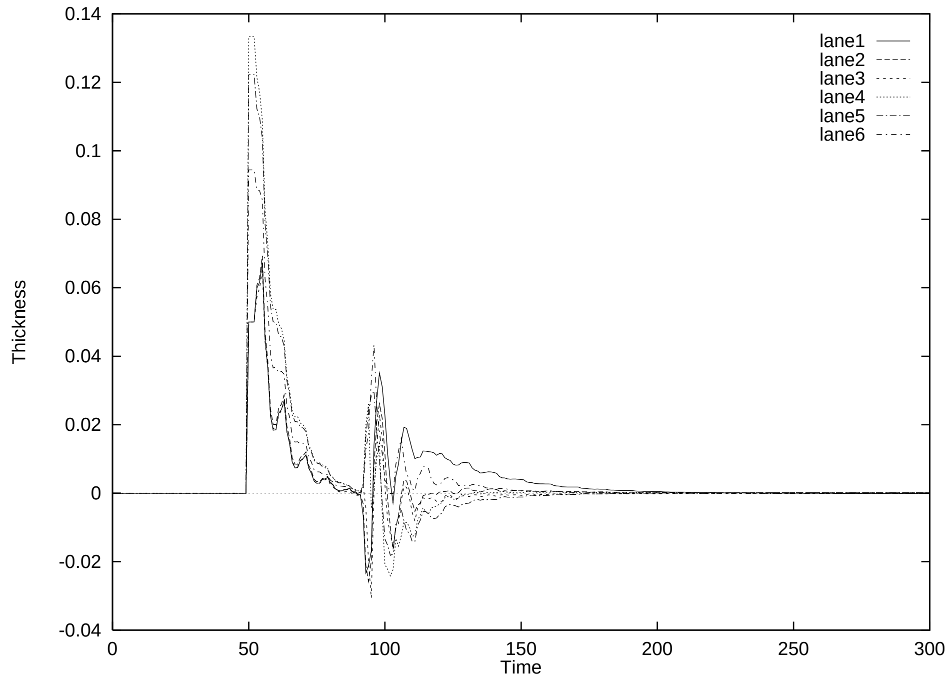

Figure 4.1: Step disturbance rejection by using two scanning sensors

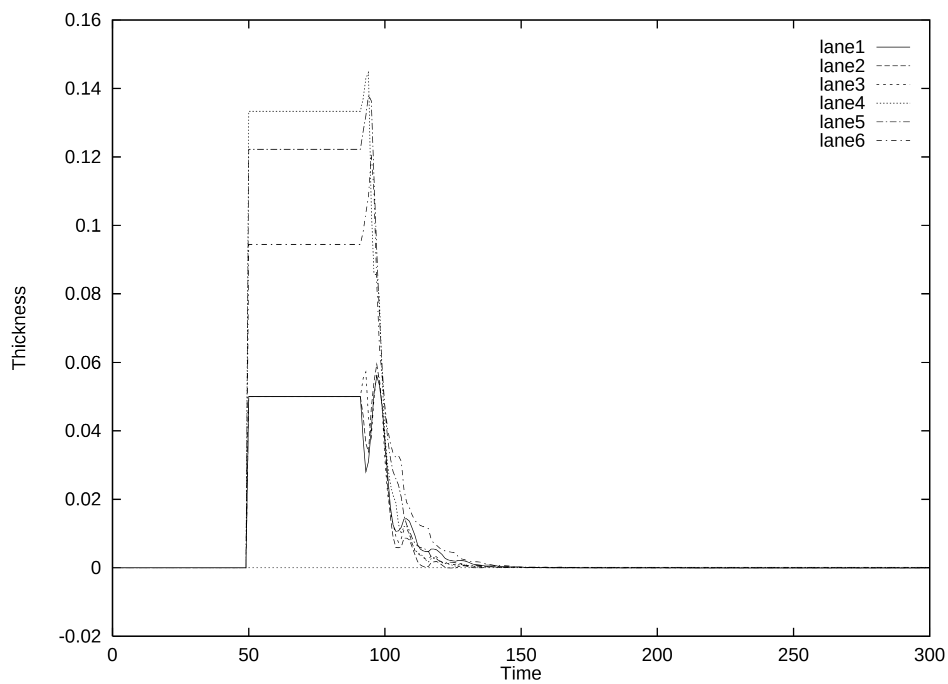

Figure 4.2: Step disturbance rejection by using one scanning sensor

Example 4.2 Consider another example. Let $p_1 = [0.2\ 0.2\ 0.2\ 0.2\ 0.2]^T$ and $p_2 = [0.117\ 0.147\ 0.167\ 0.187\ 0.187\ 0.197]^T$. Figure 4.3 shows the closed-loop response of the outputs (the thickness of 6 lanes in the wind-up position) and Figure 4.4 shows the average thickness (the MD profile). Satisfactory profiles are obtained in both the MD and the CD directions.

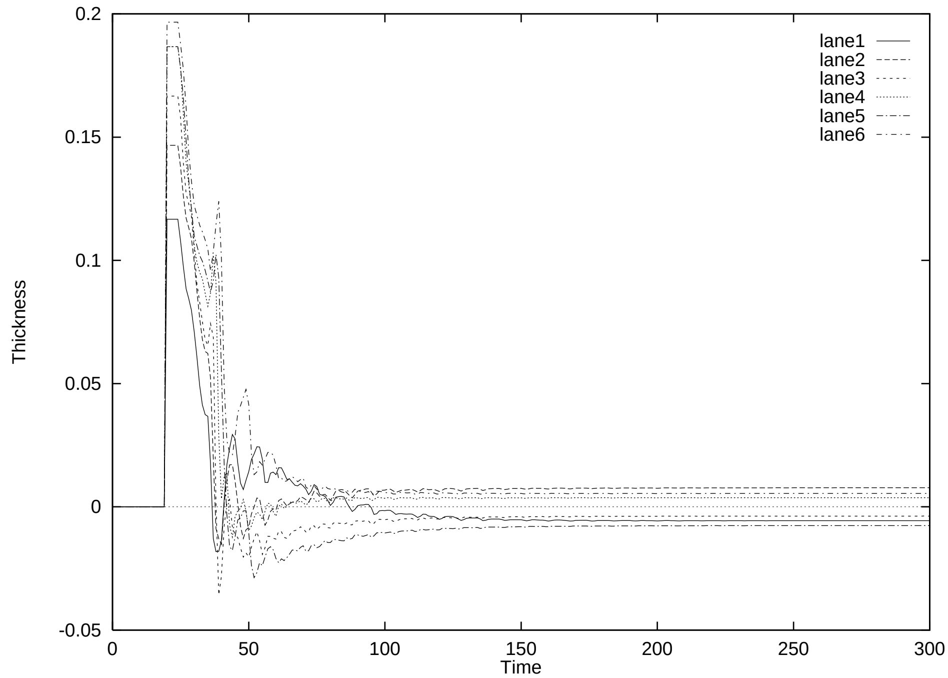

Figure 4.3: Closed-loop response of the output.

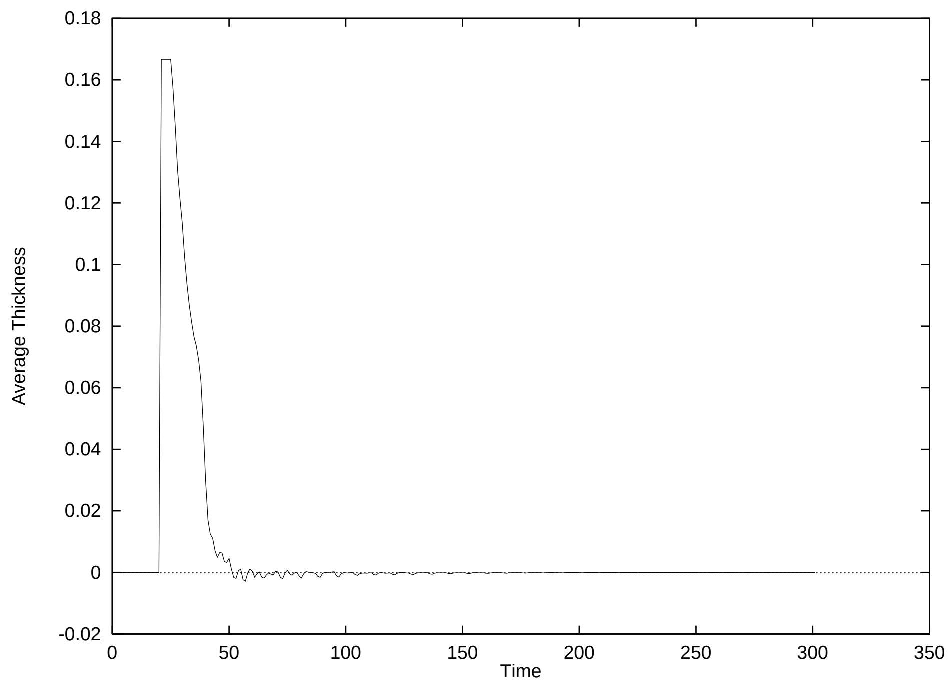

Figure 4.4: Closed-loop response of the MD profile.

Example 4.3 Now let us consider the cases when actuator faults exist. The first local actuator has a bias of 0.2 in this example. At time 10, a step disturbance occurs at the wind-up position ($p_2 = [0.05\ 0.05\ 0.05\ 0.13\ 0.12\ 0.09]^T$). Figure 4.5 shows the closed-loop response of the outputs. The actuator bias is a type of input disturbance, but acceptable performance is obtained by using an output disturbance model.

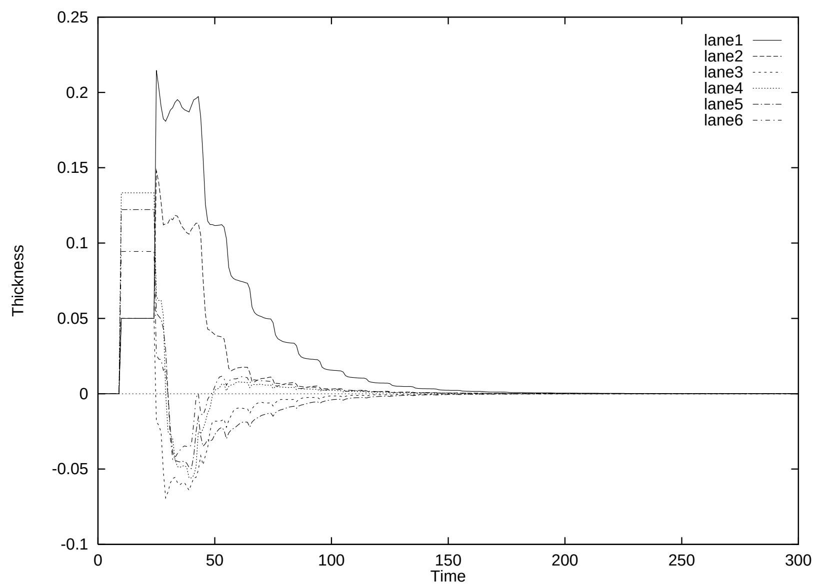

Figure 4.5: Step disturbance rejection in the case of actuator bias, without measured inputs

Example 4.4 In this example all the conditions are the same as in example two except that the first local actuator is broken instead of biased. The output profile is plotted in Figure 4.6. In this case, the controller can still reject the disturbance but is much more sluggish.

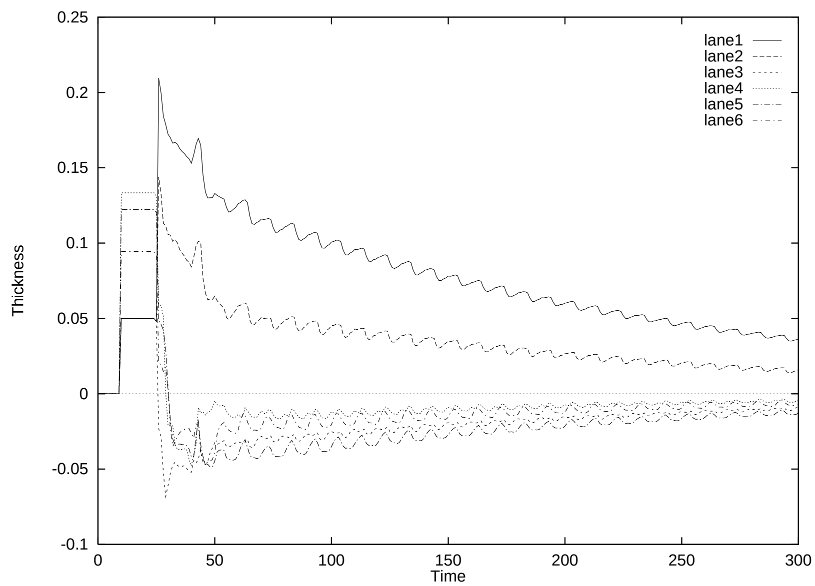

Figure 4.6: Step disturbance rejection in the case of actuator break, without measured inputs

Example 4.5 In this example we measure all the inputs and reconsider the case in example 2. Because we have more measurements, we can incorporate both input disturbance and output disturbance into our model. The closed-loop response of the outputs is plotted in Figure 4.7. The input bias is quickly detected and the output disturbances are rejected more quickly.

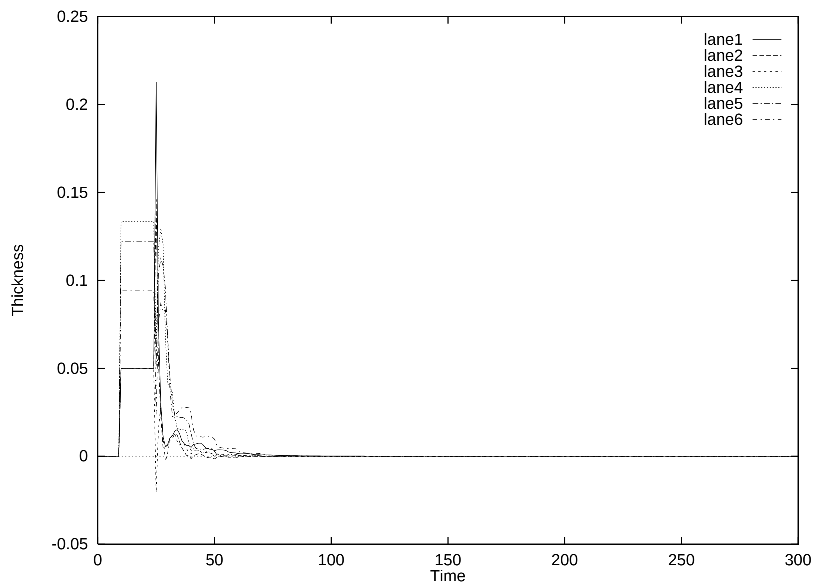

Figure 4.7: Step disturbance rejection in the case of actuator bias, with measured inputs

Example 4.6 The greatest advantage of measuring inputs is in the case of a broken actuator. In this example we reconsider the case in example 3 with measured inputs. The closed-loop response of the outputs is plotted in Figure 4.8. Compared with figure 4.6, significant improvement is achieved by measuring the inputs.

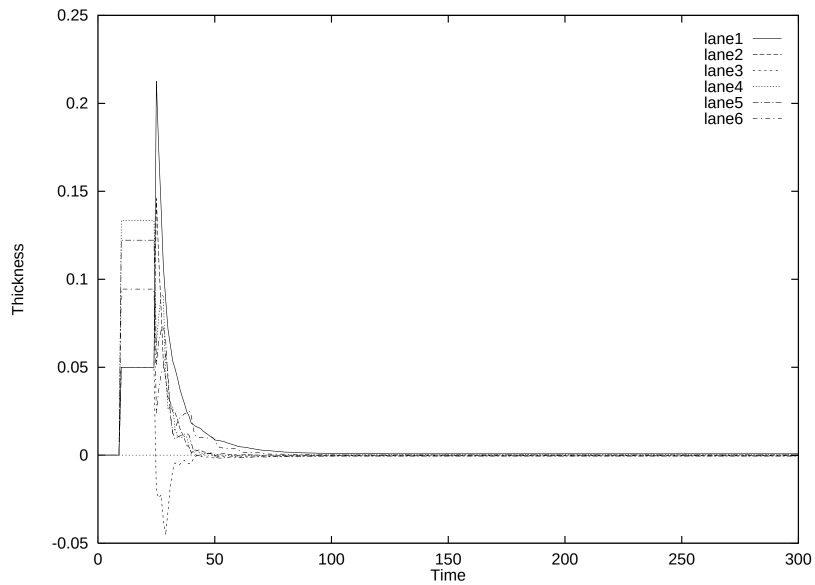

Figure 4.8: Step disturbance rejection in the case of actuator break, with measured inputs

Example 4.7 Figure 4.9 shows a case when there is a model-plant mismatch. The MPC controller use the same model as in the previous examples, but the plant model is generated by adding noises to the former model. Here

$$K_{1p} = \begin{bmatrix} 4.30 & -1.03 & -1.07 & -1.07 & -1.20 \\ -0.98 & 4.10 & -0.97 & -1.09 & -1.07 \\ -1.10 & -1.03 & 4.57 & -0.98 & -1.10 \\ -0.94 & -1.11 & -0.88 & 3.83 & -1.06 \\ -0.97 & -1.02 & -1.02 & -0.86 & 3.97 \end{bmatrix}$$

$$K_{2p} = \begin{bmatrix} 0.933 & 0.102 & -0.223 & -0.374 & -0.430 \\ 0.579 & 0.388 & -0.155 & -0.374 & -0.423 \\ -0.319 & 0.502 & 0.661 & -0.362 & -0.406 \\ -0.312 & -0.368 & 0.677 & 0.459 & -0.405 \\ -0.293 & -0.364 & -0.133 & 0370 & 0.438 \\ -0.292 & -0.359 & -0.203 & 0.111 & 0.774 \end{bmatrix}$$

This example demonstrates that the MPC controller can achieve good performance even in the case of model mismatch.

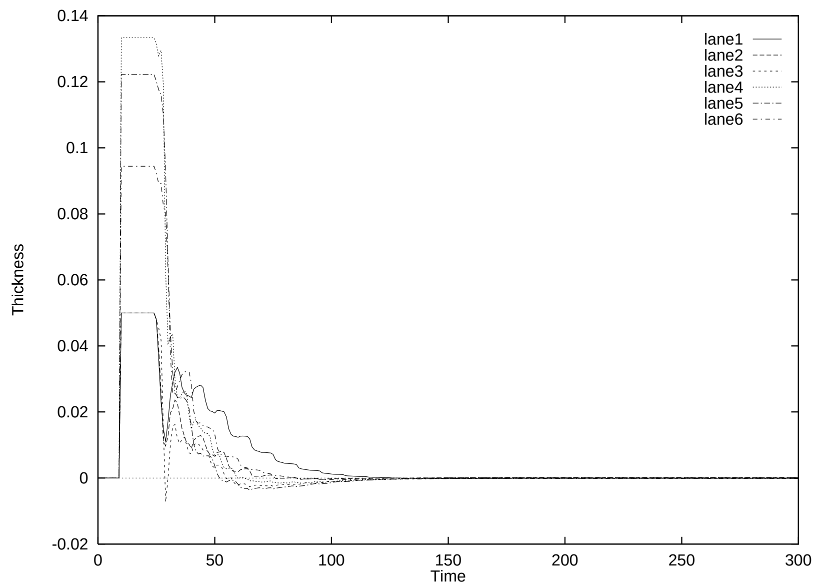

Figure 4.9: Step disturbance rejection with model/plant mismatch (1)

Example 4.8 Figure 4.10 shows another example when there is a model-plant mismatch. This example tries to simulate the case when the model mismatch is caused by unbalanced stress on the film web. The plant model is generated by letting $K_{2p} = TK_{2m}$; where K_{2p} is used to generate the output, K_{2m} is used in QP calculation and state estimation, and

$$T = \begin{bmatrix} 1 & 0 & 0 & 0 & 0 & 0 \\ 0 & 1 & 0.2 & 0.1 & 0 & 0 \\ 0 & 0 & 0.8 & 0 & 0 & 0 \\ 0 & 0 & 0 & 0.9 & 0 & 0 \\ 0 & 0 & 0 & 0 & 1 & 0 \\ 0 & 0 & 0 & 0 & 0 & 1 \end{bmatrix}$$

Again, satisfactory performance is obtained.

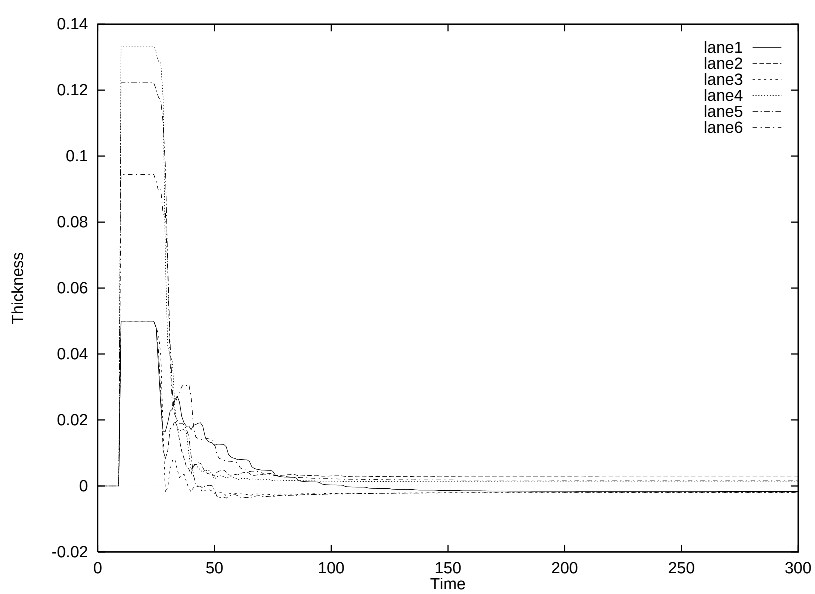

Figure 4.10: Step disturbance rejection with model/plant mismatch (2)

In this chapter we have illustrated the performance of the MPC controller under several types of disturbances. These types of disturbances are very common in the sheet and film forming processes. We have made many simulations to combine these disturbances in different models. Our simulations show that the model predictive control scheme we use is indeed an ideal control scheme for the sheet and film-forming processes.

Another type of disturbance, the lane shift, is not discussed in this chapter; we will discuss it in detail in Chapter 5.

Chapter 5

Lane Shift

This Chapter deals with lane shift, which is not considered in the previous chapters. The lane shift problem refers to the cross-directional movement of the entire sheet or film web. Discussion of this issue is not available in the literature. We will discuss how the lane shift affects the performance of the MPC controller and propose a solution to this problem.

5.1 Lane Shift

Consider the process mode

$$\begin{aligned} x(k+1) &= Ax(k) + Bu(k) \\ y(k) &= Cx(k) \end{aligned}$$

When lane shift occurs, matrices A and B will not change, but matrix C will change with the lane shift. Let us illustrate a lane shift by way of a simple four-lane example with a row of fixed sensors (See Figure 5.1).

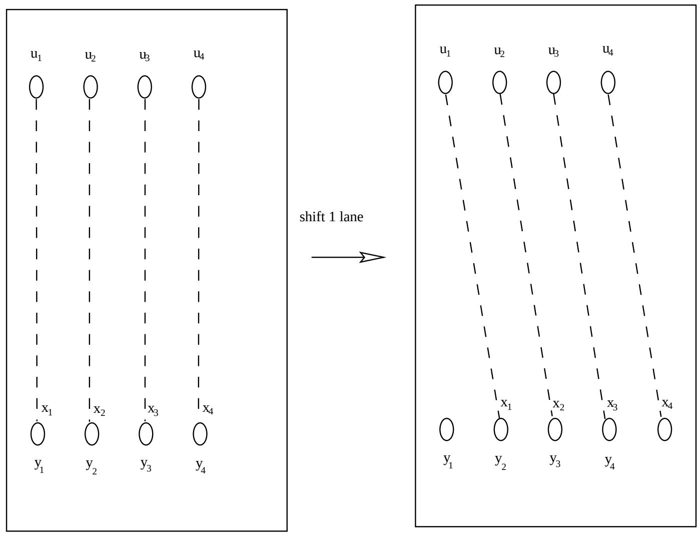

Figure 5.1: Illustration of lane shift

Without lane shift, the C matrix is

$$C = \begin{bmatrix} 1 & 0 & 0 & 0 \\ 0 & 1 & 0 & 0 \\ 0 & 0 & 1 & 0 \\ 0 & 0 & 0 & 1 \end{bmatrix}$$

If we define the distance between adjacent lanes as 1 and let the direction towards the larger lane numbers be positive, then when lane shift equals 1, the C matrix changes to

$$C = \begin{bmatrix} ? & ? & ? & ? \\ 1 & 0 & 0 & 0 \\ 0 & 1 & 0 & 0 \\ 0 & 0 & 1 & 0 \end{bmatrix}$$

Here the question marks mean that the relation between the readings of the first sensor and the states is uncertain. In the case of real systems, empirical models can usually be obtained for describing the relationship.

When the lane shift is not an integer, the C matrix can be modeled by assuming that the linear combination is reasonable. For example, if the lane shift equals 0.6, C matrix can be modeled as

$$C = \begin{bmatrix} ? & ? & ? & ? \\ 0.6 & 0.4 & 0 & 0 \\ 0 & 0.6 & 0.4 & 0 \\ 0 & 0 & 0.6 & 0.4 \end{bmatrix}$$

Extending this description to augmented state equation and scanning sensor(s) is straightforward.

Example 5.1 Because lane shift occurs in industrial operations, it is necessary to study how lane shift affects the performance of the MPC controller. Figure 5.2 is an illustration of when the process has a lane shift of 0.5 while the process has the same model and the same step disturbance as in the example 4.6 in chapter 4. The output profile is not obviously deteriorated.

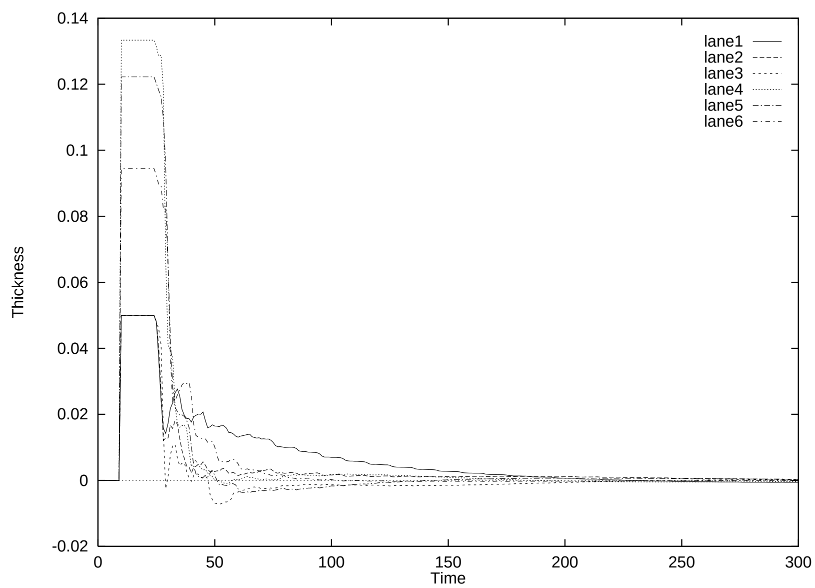

Figure 5.2: Disturbance rejection with step disturbance, white noise and lane shift=0.5.

Example 5.2 However, Figure 5.3 shows that if the lane shift is large enough, the system may become unstable due to large model mismatch. In this example, the lane shift equals 1 and an unstable saw-tooth shape profile is observed. This example demonstrates the necessity to identify large lane shift and adjust the regulator appropriately.

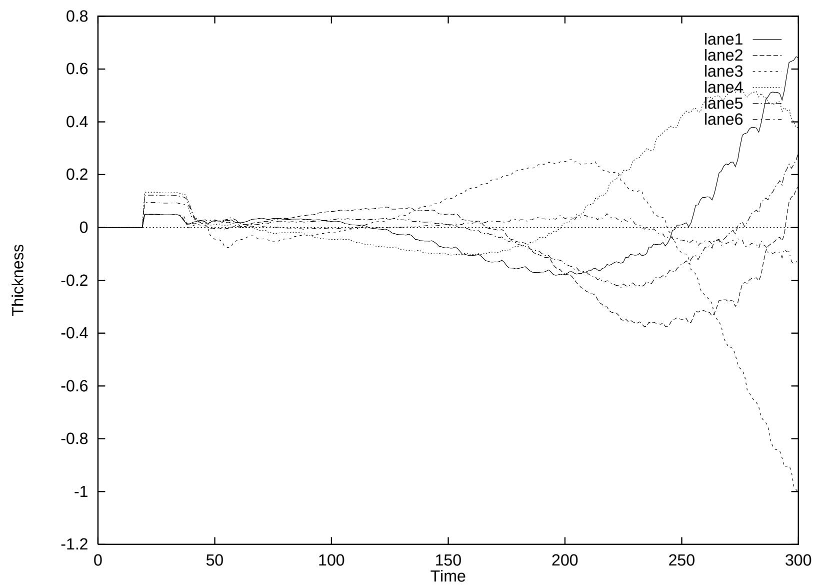

Figure 5.3: Disturbance rejection with step disturbance, white noise and lane shift=1.

5.2 Lane identification

We have showed that lane shift may cause the MPC controller to become unstable. When one model cannot give satisfactory result, we should consider using another model that is more accurate. Assume the thickness outside the lanes can be modeled as the same as that of the nearest lane, for a five-lane example, if lane shift equals 1, the best choice for C matrix is

$$C = \begin{bmatrix} 1 & 0 & 0 & 0 & 0 \\ 1 & 0 & 0 & 0 & 0 \\ 0 & 1 & 0 & 0 & 0 \\ 0 & 0 & 1 & 0 & 0 \\ 0 & 0 & 0 & 1 & 0 \end{bmatrix}$$

Since we cannot predict when lane shift occurs and how much the shift will be, we have to identify it on-line. Fortunately, lane shift is physically limited, and small model mismatch will not deteriorate the performance. Therefore it is practical for us to select an appropriate model from only a small number of candidates.

Consider a set of models $\{C_1, C_2, \ldots, C_r\}$, whose elements relate to different lane shifts, and where r is the number of model candidates. A set of Kalman filter gains $\{L_1, L_2, \ldots, L_r\}$ can then be calculated, with L_i corresponding to C_i. (C_i and L_i can be time-varying.) If we assume a set of initial state estimates $\{\hat{x}_1(0), \hat{x}_2(0), \ldots, \hat{x}_r(0)\}$, a sequence of input $u(0), u(1), \ldots$, and a sequences of outputs $y(0), y(1), \ldots$, then two matrices X and E can be obtained by using the following formula:

$$\begin{aligned} X_{i,k} &= AX_{i,k-1} + Bu(k) + L_i(k)\left(y(k) - C_i(k)X_{i,k-1}\right) \\ E_{i,k} &= y(k) - C_i(k)X_{i,k-1} \\ X_{i,1} &= \hat{x}_i(0) \end{aligned}$$

If $u(k), y(k)$ represent the inputs and outputs of a real process that can be modeled by

$$\begin{aligned} x(k+1) &= Ax(k) + Bu(k) \\ y(k) &= C_q x(k) \qquad\qquad (1 \leq q \leq r) \end{aligned}$$

then according to the property of Kalman filter, $E_{q,k} \to 0$ as $k \to \infty$. If white noise is considered, $\{E_{q,k-w}, \ldots, E_{q,k-1}, E_{q,k}\}$ approaches a zero mean sequence as $k \to \infty$; here w is a time horizon. Note the input sequence $\{\ u(k)\ \}$ can be arbitrary. Even in the case when the $u(k)$ sequence leads to unstable performances, $E_{q,k}$ still approaches a zero mean sequence. See the following examples.

Example 5.3 Consider an example of a 10-lane process. The plant model is

$$\begin{aligned} x(k+1) &= Ax(k) + Bu(k) \\ y(k) &= C_0 x(k) + C_0 p(k) + v(k) \end{aligned}$$

where $p(k)$ is output disturbance and $v(k)$ is white noise. At time 0, step disturbances occur in lanes 2, 3, 4 with amplitude 0.05, 0.1, 0.04 respectively. Let $C_{-2}, C_{-1}, C_0, C_1, C_2$ represent C matrices corresponding

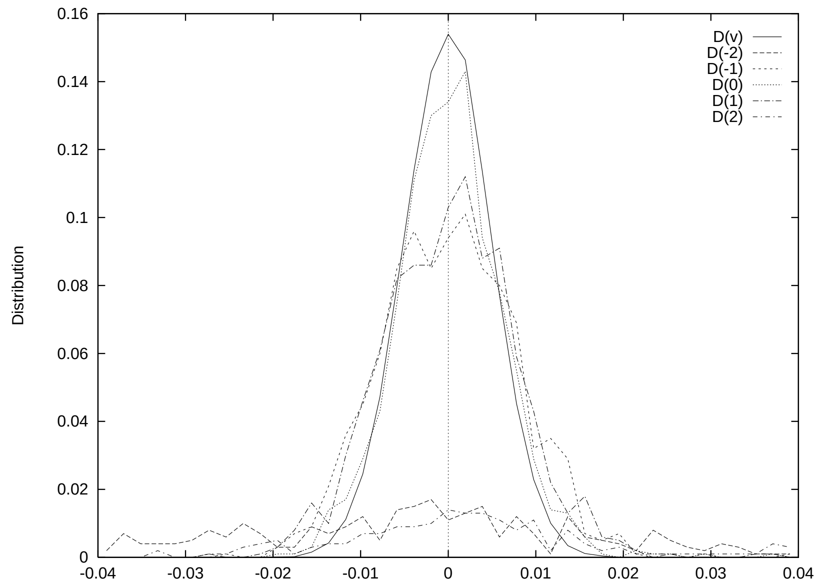

Figure 5.4: distribution of errors when shift=0

to lane shift of $-2, -1, 0, 1, 2$ respectively. While the MPC controller uses the correct model (C_0) to reject these disturbances, we use all five models to estimate the states and disturbances separately. The distributions of the estimate errors are plotted in Figure 5.4. Figures 5.5 and 5.6 show the sum of the square errors in a fixed moving horizon ($W = 14$). $E_i(k)$ corresponds to model $C_i(k)$. We see while E_{-2} and E_2 become bigger and bigger, E_{-1}, E_0, E_1 approach small mean normal distributions.

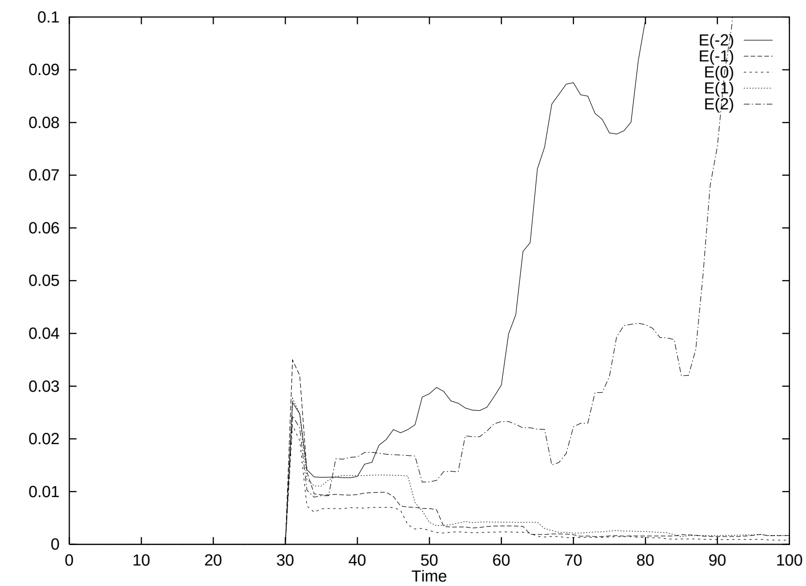

Figure 5.5: Accumulated errors when shift=0, t=1:250

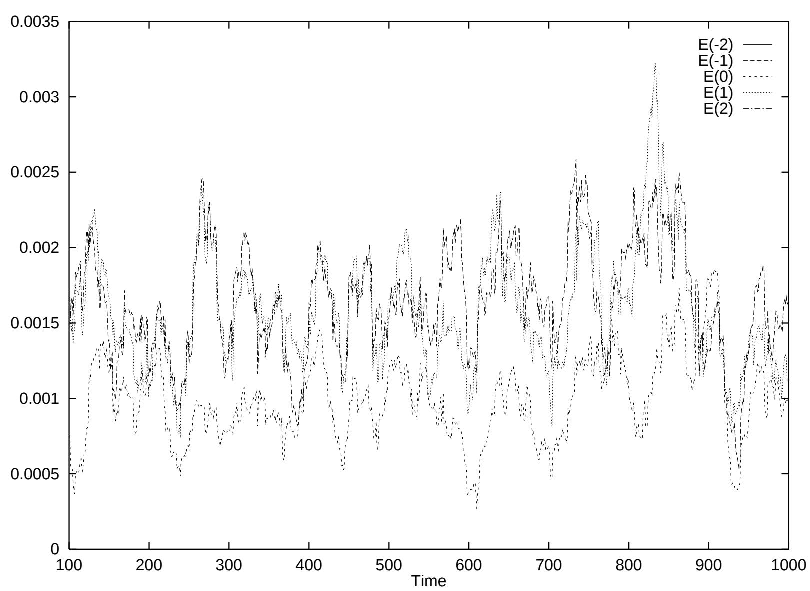

Figure 5.6: Accumulated errors when shift=0, t=251:1000

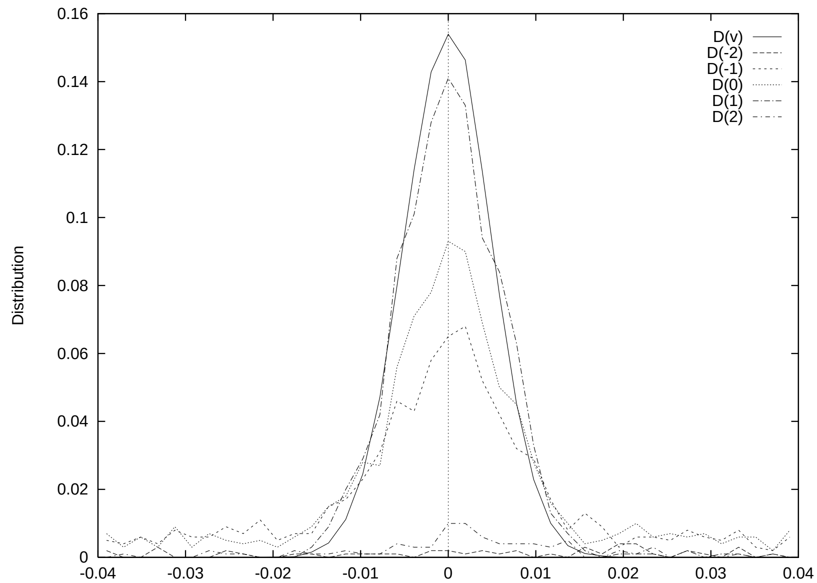

Figure 5.7: distribution of errors when shift=1

Example 5.4 Now let the plant have one lane shift:

$$
\begin{aligned}
x(k+1) &= Ax(k) + Bu(k) \\
y(k) &= C_1 x(k) + C_1 p(k) + v(k)
\end{aligned}
$$

We still use C_0 as the MPC model and use all five models to estimate states and disturbances. The distributions of the estimate errors are plotted in Figure 5.7. The sum of the square errors in a fixed moving horizon ($W = 14$) are plotted in Figures 5.8 and 5.9. This time the MPC controller uses an incorrect model, only E_1 doesn't go up quickly. E_0 returns to small numbers because the process ends in a steady state, a state far from our setpoint.

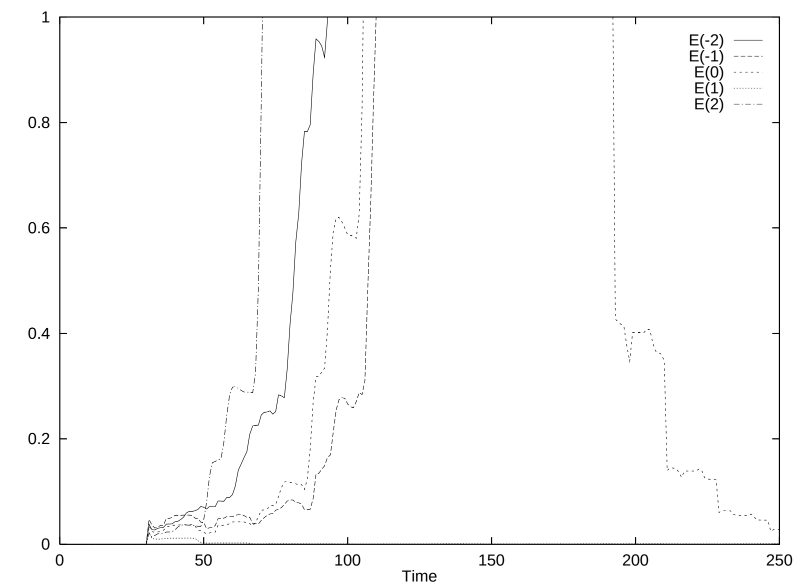

Figure 5.8: Accumulated errors when shift=1, t=1:250

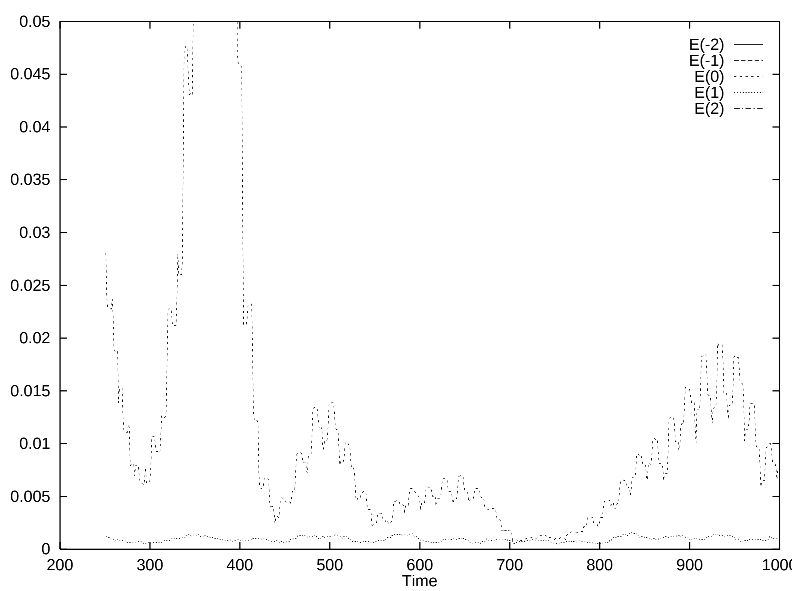

Figure 5.9: Accumulated errors when shift=1, t=251:1000

The above simulations suggest the following lane shift identification method:

- step 1: Given a set of plant models, calculate a set of Kalman Filter gains.
- step 2: Assume initial values and MPC model.
- step 3: Solve QP problem using the MPC model.
- step 4: State estimation separately.
- step 5: Compare with sensor measurement.
- step 6: Update the MPC model.
- step 7: Repeat steps 3 to 7.

In step 1, we choose several models ($\{C_{-r}, \ldots, C_0, \ldots, C_r\}$) as the candidate models and calculate a set of Kalman filter gains corresponding to each candidate model. This step is off-line. Step 2 is the start step for the controller. This step provides all the initial conditions and a model for the first QP problem. Step 3 is the QP step, in which an optimal input sequence is calculated and the first is injected into the process. In step 4 we use each candidate model to estimate the state, the output, and the disturbance separately. In step 5, the sensor measurement is compared with each estimation and the square errors are pushed into the matrix that stores the square errors in a fixed length moving horizon. In step 6, a criterion is used to update the MPC model if necessary. Then we return to step 3 and the procedure is repeated.

The criterion in step 6 is the following:

Let $C_a(-r \leq a \leq r)$ be the selected optimal model at time k-1; if

$$\min_i \sum_{j=k-w+1}^{k} E_i^2(j) \ \leq \ \sum_{j=k-w+1}^{k} E_a^2(j) - M$$

then select C_b as the optimal model at time k. Here W is the length of the moving horizon, M is a nonnegative real number, and

$$b = arg \min_i \sum_{j=k-w+1}^{k} E_i^2(j)$$

When $M = 0$, the assumed optimal model always has a minimal sum of square errors between estimates and sensor readings, but it may lead the MPC controller to change the optimal model too frequently and deteriorate the performance. A positive M can prevent such mis-selection of the optimal model. Sometimes more than one model can lead to good performance. If one model can satisfactorily control the process, it is not necessary to replace it with a more accurate model. When $M = \infty$, the controller becomes the normal MPC controller. The M chosen should be small enough to guarantee quick response to significant lane shift, but big enough to decrease the possibility of incorrect model selection. The length of horizon W can also affect the controller's performance. Because a large W will increase the calculation burden and delay response to significant lane shift, it is better to choose a small W.

5.3 Examples

The following examples show how the method works when we incorporate lane identification into our MPC scheme.

Example 5.5 Consider the case in example 5.2. Figures 5.10 and 5.11 show that the system becomes stable and satisfactory performance is obtained due to the lane identification.

Example 5.6 Keeping all the conditions, we change the lane shift from 1 in example 5.5 to 0.8. The exact model for lane shift that equals 0.8 is not included in the set of candidate models; however, good results can still be obtained as shown in Figures 5.12 and 5.13.

Example 5.7 In this example we let the lane shift be a sinusoid function. This is similar to the case when the lane shift changes slowly in the real processes. Figures 5.14 and 5.15 show that our method works well in these cases. White noise is generated in the simulation.

These examples illustrate that the identification method we use here is effective in identifying significant lane shifts in the sheet and film forming processes. More simulations have been done to verify reliability. Other types of disturbances, such as actuator faults, are also investigated and results similar to the above example are obtained.

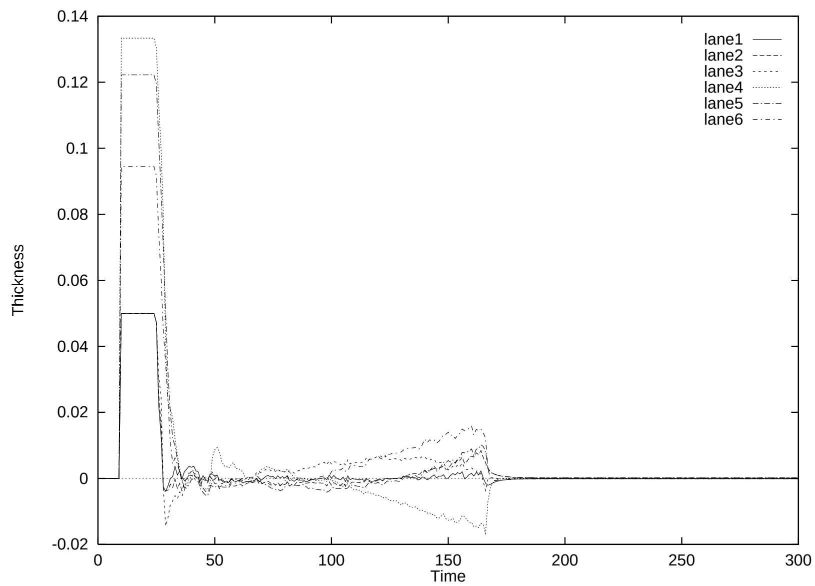

Figure 5.10: Disturbance rejection with step disturbance, white noise and lane shift=1.

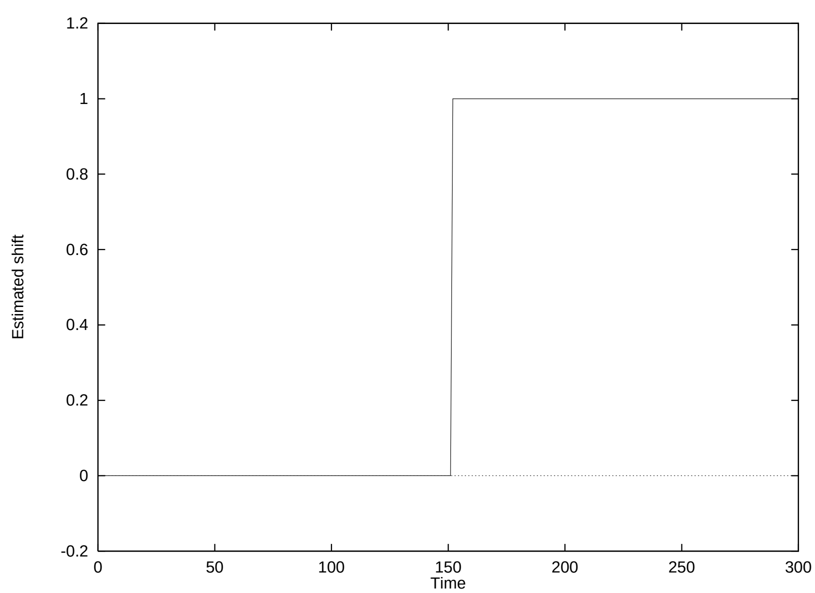

Figure 5.11: Disturbance rejection with step disturbance, white noise and lane shift=1.

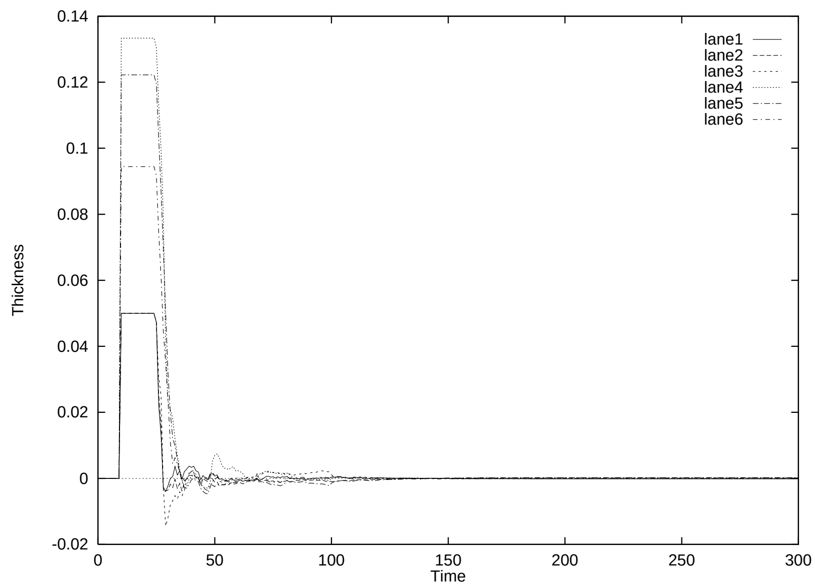

Figure 5.12: Disturbance rejection with step disturbance, white noise and lane shift=0.8.

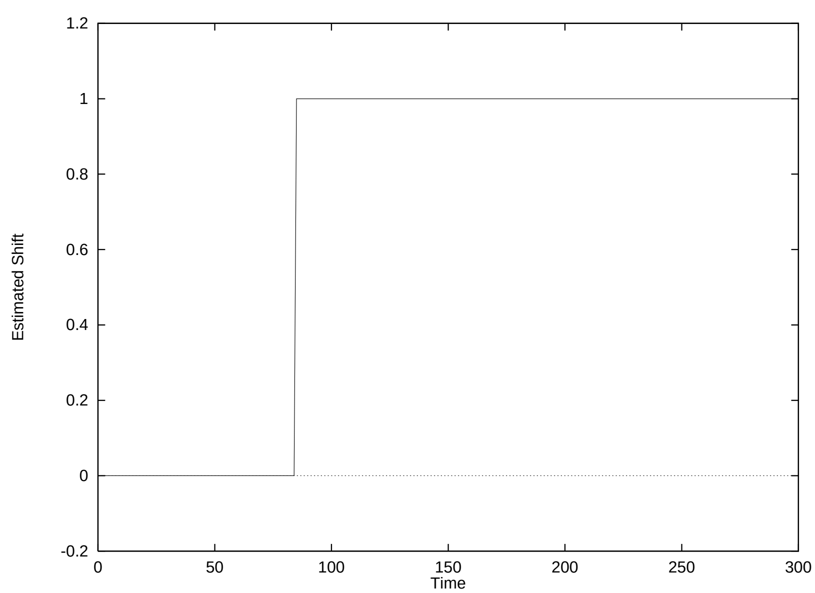

Figure 5.13: Disturbance rejection with step disturbance, white noise and lane shift=0.8.

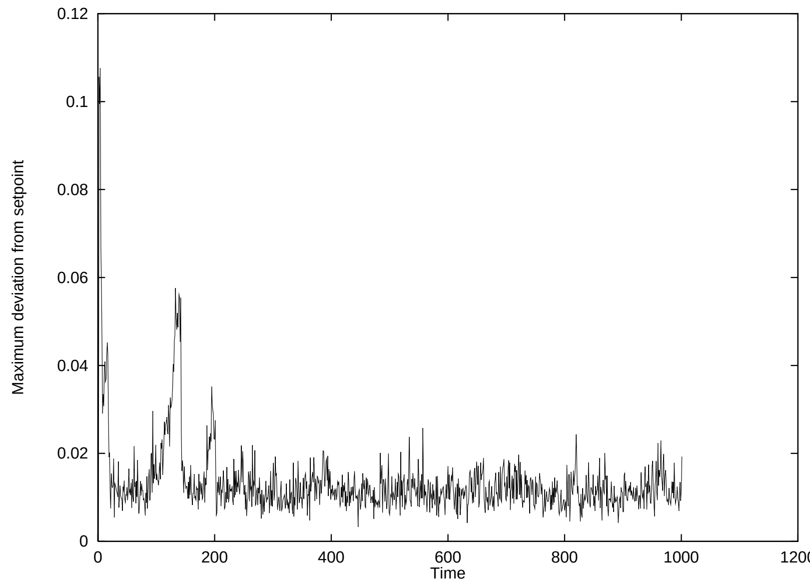

Figure 5.14: Disturbance rejection with step disturbance, white noise and lane shift changes as a sinusoid function.

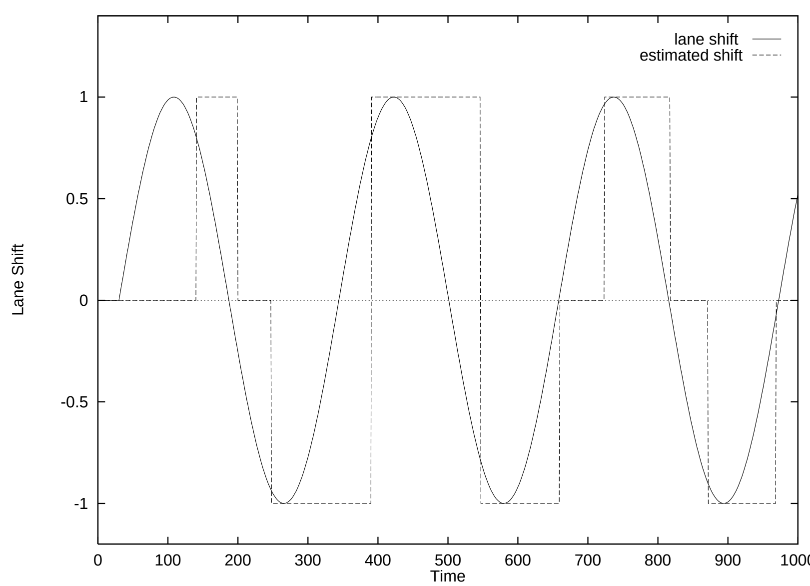

Figure 5.15: Disturbance rejection with step disturbance, white noise and lane shift changes as a sinusoid function.

Chapter 6

Conclusions

The goal of this research is to apply model predictive control to the gage control problem. Although the nominal stability of this MPC algorithm has been established, the robust stability problem has not been well studied. Robust stability is a serious concern in industrial MPC applications and is currently addressed through the use of extensive closed loop simulation prior to implementation. One task of this research is to test our MPC algorithm under various combinations of possible disturbances and anticipate its practicability in industry. Another task is to study possible new strategies to improve control. These strategies include using an additional scanning sensor, measuring inputs, and simultaneously controlling MD and CD variations.

The MPC scheme provides an excellent approach to the simultaneous dynamic control over both MD and CD property variations present in sheet and film forming processes. In Bergh's words, "although decoupled MD and CD control problems often can be justified in practice, this more general coupled approach should allow for improved control." This remark is supported by our simulation results. Our method need not reconstruct MD and CD variations, and good performance is observed to reject both variations.

Large dimension and large time delay are important characteristics of the sheet and film forming processes. Our algorithm discards time delay in the optimization step and therefore greatly reduces the computation of solving the quadratic optimization problem. Another problem with time delay is that some disturbances cannot be detected until they come to the end of the process after a long time delay. We have showed improvement can be made by adding another scanning sensor at the casting position. This sensor can quickly detect disturbances at the casting position and upstream of this position, making the controller reject these disturbances much earlier. The bigger the time delay, the more the improvement. Because our scheme optimizes only the final profile, the optimization problem will not be enlarged by additional measurement.

We have also demonstrated the advantage of measuring the inputs. Without measuring the inputs, the MPC controller can compensate for actuator faults, but it is quite sluggish in the case of a broken actuator. Measuring the inputs can make significant improvement, deduce the maximal deviation from the setpoint, and reject disturbances quickly.

Our algorithm is tested under various combinations of important disturbances that might happen in practice. Simulation results show that the controller we use provides satisfactory performance even when there exists model mismatch, equipment faults and various disturbances. One case in which the closed-loop system may become unstable in practice would be when large lane shift occurs. This problem is solved by incorporating an on-line identification scheme into the ordinary MPC controller. This method guarantees the stability of the closed-loop systems and makes the controller adaptive and robust. It is different from most of the robust MPC schemes under current research in that the optimization problem is not changed. Most approaches currently under development are based on solving the nominal MPC problem with an additional constraint to ensure robust stability [4, 27, 23]. Taking into account the large-scale characteristic of the sheet and film forming processes, the simplicity of the optimization problem in our method seems to have significant advantages. Performance is improved without additional constraint on the optimization. The method also provides flexibility of the nominal optimization algorithm.

The MPC scheme with on-line identification is tested by simulations that consider various possible disturbances. Simulation results demonstrate that the scheme can control simultaneously MD and CD profiles and that good performance can be obtained in the case where various types of disturbances, actuator faults and model mismatch occur in the systems. The approach is general and can be used to handle different processes using multiple sensors and multiple actuators. It is possible to reduce the computational load based on specific characteristics of the process model. More effective on-line identification methods can also be developed. The scheme is expected to be tested on a production line in the future.

Bibliography

[1] Yaman Arkun and Ferhan Kayihan. Identification of full profile disturbance models for sheet forming processes. *Accepted for Publication in* AICHE Journal, 1996.

[2] K. J. Åström. Computer control of a paper machine – an application of linear stochastic control theory. *IBM J. Res. Dev.*, 11:389–405, 1967.

[3] Karl J. Åström. *Introduction to Stochastic Control Theory*. Academic Press, San Diego, California, 1970.

[4] Thomas A. Badgwell. Robust stability constraints for model predictive control: A unifying review and some new results. Presented at the 1996 AICHE meeting, Chicago, Illinois, Paper 1141, 1996.

[5] A. E. Beecher and R. A. Bareiss. Theory and practice of automatic control of basis weight profiles. *Tappi*, 53(5):847–852, May 1970.

[6] Luis G. Bergh and John F. MacGregor. Spatial control of sheet and film forming processes. *The Canadian Journal of Chemical Engineering*, 65:148–155, February 1987.

[7] Thomas J. Boyle. Control of cross-direction variations in web forming machines. *The Canadian Journal of Chemical Engineering*, 55:457–461, August 1977.

[8] Thomas J. Boyle. Practical algorithms for cross–direction control. *Tappi Journal*, 61:77–80, January 1978.

[9] Richard D. Braatz, Babatunde A. Ogunnaike, and Andrew P. Featherstone. Control of sheet and film processes – a critical review. Submitted to Automatica, February 1995.

[10] Richard D. Braatz, Matthew L. Tyler, Manfred Morari, Ferdinand R. Pranckh, and Luigi Sartor. Identification and cross-directional control of coating processes. *AIChE Journal*, 38(9):1329–1339, 1992.

[11] Donald B. Brewster and Andrew K. Bjerring. Computer control in pulp and paper 1961–1969. *Proceedings of the IEEE*, 58(1):49–69, January 1970.

[12] A. E. Bryson and Y. Ho. *Applied Optimal Control*. Hemisphere Publishing, New York, 1975.

[13] Dae Gyu Byun and Wook Hyun Kwon. Predictive control: A review and some new stability results. In T. J. McAvoy, Y. Arkun, and E. Zafiriou, editors, *Proceedings of the 1988 IFAC Workshop on Model Based Process Control*, pages 81–87, Oxford, 1988. Pergamon Press.

[14] John C. Campbell and James B. Rawlings. Estimation and control of sheet and film forming processes. In Irena Lasiecka and Blaise Morton, editors, *Control Problems in Industry*, pages 43–63, Boston, 1995. SIAM, Birkhäuser.

[15] John C. Campbell and James B. Rawlings. Identification and control of sheet forming processes. In *Proceedings of the 13th IFAC World Congress*, San Francisco, California, July 1996.

[16] S. C. Chen. Kalman filtering applied to sheet measurement. In *Proceedings of the American Control Conference*, Atlanta, GA, June 1988.

[17] S. C. Chen and R. G. Wilhelm, Jr. Optimal control of cross-machine direction web profile with constraints on the control effort. In *Proceedings of the American Control Conference*, Seattle, WA, June 1986.

[18] R. M. C. De Keyser, G. A. Van de Velde, and F. A. G. Dumortier. A comparative study of self-adaptive long-range predictive control methods. *Automatica*, 24(2):149–163, 1988.

[19] Guy A. Dumont. Application of advanced control methods in the pulp and paper industry – A survey. *Automatica*, 22:143–153, 1986.

[20] Guy A. Dumont, Ivar Mar Jonsson, Michael S. Davies, Fariborz T. Ordubadi, Ye Fu, K. Natarajan, Claes Lindeborg, and E. Michael Heaven. Estimation of moisture variations on paper machines.

IEEE Transactions on Control Systems Technology, 1(2):101–113, June 1993.

[21] J.W. Eaton and J.B. Rawlings. Octave—a high-level interactive language for numerical computations. *CACHE News*, (40): 11-18, Spring 1995.

[22] Carlos E. García, David M. Prett, and Manfred Morari. Model predictive control: Theory and practice—a survey. *Automatica*, 25(3):335–348, 1989.

[23] H. Genceli and M. Nikolaou. New approach to constrained predictive control with simultaneous model identification. *AIChE Journal*, 42(10):2857–2866, October 1996.

[24] E. M. Heaven, T. M. Kean, I. M. Jonsson, M. A. Manness, K. M. Vu, and R. N. Vyse. Applications of system identification to paper machine model development and controller design. In *Second IEEE Conference on Control Applications*, pages 227–233, Vancouver, B.C., September 1993.

[25] Kristinn Kristinsson and Guy A. Dumont. Paper machine cross directional basis weight control using gram polynomials. In *Second IEEE Conference on Control Applications*, pages 234–240, Vancouver, B.C., September 1993.

[26] Jay H. Lee. Recent advances in model predictive control and other related areas. Fifth International Conference on Chemical Process Control, Lake Tahoe, California, January 1996.

[27] David Q. Mayne. Nonlinear model predictive control: an assessment. Fifth International Conference on Chemical Process Control, Lake Tahoe, California, January 1996.

[28] Kenneth R. Muske. *Linear Model Predictive Control of Chemical Processes*. PhD thesis, The University of Texas at Austin, 1995.

[29] Kenneth R. Muske and James B. Rawlings. Model predictive control with linear models. *AIChE Journal*, 39(2):262–287, 1993.

[30] S. Joe Qin and Thomas A. Badgwell. An overview of industrial model predictive control technology. Fifth International Conference on Chemical Process Control, Lake Tahoe, California, January 1996.

[31] James B. Rawlings and I-Lung Chien. Gage control of film and sheet-forming processes. *AIChE Journal*, 42(3):753–766, March 1996.

[32] James B. Rawlings, E. Scott Meadows, and Kenneth R. Muske. Nonlinear model predictive control: A tutorial and survey. In *ADCHEM '94 Proceedings, Kyoto, Japan*, 1994.

[33] James B. Rawlings and Kenneth R. Muske. Stability of constrained receding horizon control. *IEEE Transactions on Automatic Control*, 38(10):1512–1516, October 1993.

[34] Pierre O.M. Scokaert and James B. Rawlings. Stability of model predictive control under perturbations. In *IFAC Symposium on Nonlinear Control System Design, Tahoe City, California*, pages 21–26, 1995.

[35] M. L. Tyler and M. Morari. Estimation of cross directional properties: Scanning versus stationary sensors. *AIChE Journal*, 41(4):846–854, April 1995.

[36] Xiaochun George Wang, Guy A. Dumont, and Michael S. Davies. Adaptive basis weight control in paper machines. In *Second IEEE Conference on Control Applications*, pages 209–216, Vancouver, B.C., September 1993.

[37] Xiaochun George Wang, Guy A. Dumont, and Michael S. Davies. Estimation in paper machine control. *IEEE Control Systems*, pages 34–43, August 1993.

[38] R. G. Wilhelm, Jr. and M. Fjeld. Control algorithms for cross directional control: the state of the art. In *Proceedings of the 5th IFAC/IMEKO Conference on Instrumentation in the Paper, Rubber, Plastic and Polymerization Industries*, Antwerp, October 11-13 1983.

[39] A. J. Wilkinson and A. Hering. A new control technique for cross machine control of basis weight. In *Proceedings of the 5th IFAC/IMEKO Conference on Instrumentation in the Paper, Rubber, Plastic and Polymerization Industries*, Antwerp, October 11-13 1983.

[40] Q. Xia, M. Rao, and J. Qian. Model algorighmic control for paper machines. In *Second IEEE Conference on Control Applications*, pages 203–208, Vancouver, B.C., September 1993.